Journal of Smart Systems Research | e-ISSN: 2757-6787

Volume: 5 | Number: 1 | Year: 2024

Table of Contents

Ahmet KOLUMAN, Atakan KONUKBAY

Decontaminants Used After Biorisk Material Decontamination: Environmental Impact and the Role of Drones in Detection and Remediation of Resistance in Ecosystems ……..………..…1-16

Mehmet DUMAN, Volkan BERK

Geniş Bantlı Yüksek Performanslı Antipodal Vivaldi Anteni: Kablosuz İletişim Sistemleri için Verimli Bir Tasarım ………………………………………………………………………17-32

Mert Süleyman DEMİRSOY, Metin Eren ATALAY, Ardi, BILLURDAGI, Mustafa Çağrı KUTLU

A Low-Cost Soft Gripper for Automated Pick-and-Place Systems ……………………….33-39

Cem ÖZKURT

Assessing Student Success: The Impact of Machine Learning and XAI-BBO Approach ..40-54

Hamid ASADI DERESHGI, Sezer BİÇER, Özge Naz GÜRBÜZ, Dilan DEMİR

Advancements and Innovations in Elbow Orthoses: An Extensive Review of Design, Development, and Clinical Applications …………………………………...…………..55-65

Research Paper
Journal of Smart Systems Research (JOINSSR) 5(1),1-16,2024
Received: 23-October-2023 Accepted: 26-January-2024
DOI: 10.58769/joinssr.1379496

SAKARYA UNIVERSITY OF APPLIED SCIENCES

Decontaminants Used After Biorisk Material Decontamination: Environmental Impact and the Role of Drones in Detection and Remediation of Resistance in Ecosystems

Ahmet KOLUMAN[1*], Atakan KONUKBAY[2]

[1] Biomedical Engineering, Technology Faculty, Pamukkale University, Türkiye, akoluman@pau.edu.tr

[2] Havelsan CBRN Product Manager, Ankara, Türkiye, akonukbay@havelsan.com.tr

ABSTRACT

In our rapidly evolving world, the confluence of challenges and opportunities in decontamination, ecological resilience, and cutting-edge technology has become a focal point of concern and innovation. This review explores the interplay between these elements, with profound implications for human safety and environmental equilibrium. Post-decontamination treatment is pivotal in countering Chemical, Biological, Radiological, and Nuclear (CBRN) hazards. Thorough contamination elimination is imperative for risk management. The emergence and proliferation of resistance within ecosystems present a complex challenge. Resistance mechanisms can thwart decontamination agents, affecting environmental restoration, human health, and ecological resilience. Drone technology heralds a transformative era in environmental monitoring. Drones with advanced sensors and data capabilities provide access to remote, hazardous, and inaccessible ecological areas. Real-time data empowers researchers to adapt to evolving conditions, including resistance dynamics. Drones also serve as tools for targeted remediation in contaminated areas, optimizing resource allocation and minimizing disruption. Case studies highlight their efficacy in ecological restoration. Integrating drones into post-decontamination protocols is a paradigm shift. Real-time data, facilitated by drones, bridges the gap between ecological understanding and strategic action. In conclusion, safeguarding our world is a collective responsibility. Drones symbolize our commitment to harmonizing human needs with the environment. This review illuminates a path forward, celebrating our capacity to protect, preserve, and prosper, not just for ourselves but for the world we inhabit. It emphasizes the imperative to save our planet, forging a sustainable future where humanity and nature thrive in harmonious coexistence.

Keywords: Decontamination, resistance, drone technology, environmental monitoring, ecological resilience

[*]Corresponding Author's email:akoluman@pau.edu.tr

1 Introduction

In an era characterized by rapid technological advancements and an increasingly interconnected global community, the management of biorisk materials and the consequences of their inadvertent release or misuse have emerged as critical concerns for both public health and environmental preservation [1]. The process of decontamination, which seeks to mitigate the hazards posed by these materials, represents a pivotal component in safeguarding human health and ecological integrity [2]. However, it is imperative to recognize that the efficacy of decontamination procedures is not without collateral ramifications, particularly regarding their environmental implications [3].

Concurrently, the advent of drone technology has opened new vistas in environmental monitoring and remediation. Drones, equipped with advanced sensor arrays and remote sensing capabilities, offer an unprecedented opportunity to scrutinize the aftermath of decontamination efforts with precision, allowing for real-time data collection and decision-making [4]. Their integration into biorisk material management holds immense potential in addressing the ecological consequences of post-decontamination decontaminants and in developing targeted strategies for resistance detection and remediation. As traversing the intricate terrain of post-decontamination decontaminants, environmental impacts, and the pivotal role of drones, this review endeavors to elucidate the complexities surrounding these issues [5]. Through a synthesis of existing literature, analysis of case studies, and exploration of future research directions, this review seeks to provide a comprehensive understanding of the challenges and opportunities that lie at the intersection of decontamination, environmental stewardship, and the preservation of ecosystem resilience. In so doing, it underscores the imperativeness of adopting a holistic approach that harmonizes human safety with environmental sustainability in the context of biorisk material management [6].

This review aims to delve into the intricate and multifaceted nexus between post-decontamination decontaminants, their influence on the environment, and the evolving challenges posed by the emergence of resistance in ecosystems. While the immediate objective of decontamination is to render biorisk materials innocuous, the inherent properties of decontaminants and their interaction with environmental matrices often engender unforeseen ecological perturbations [7]. In parallel, the phenomenon of resistance, long studied within the realm of antimicrobial resistance, is increasingly manifesting itself in ecological settings post-decontamination, eliciting concerns about the resilience of ecosystems and their capacity to rebound from anthropogenic perturbations [8].

2 Post-Decontamination Decontaminants: Agents and Their Environmental Implications

The effective mitigation of biorisk materials necessitates not only the initial decontamination procedures but also the subsequent application of post-decontamination decontaminants [9]. These agents, designed to neutralize residual contamination and ensure the complete eradication of hazardous materials, play a pivotal role in the safety and security of both human populations and the environment [10,11].

2.1 Types of Post-Decontamination Decontaminants

Post-decontamination decontaminants encompass a spectrum of chemical, biological, and physical agents, each tailored to the specific nature of the biorisk material and the environment in which decontamination occurs. These agents are diverse, ranging from oxidizing chemicals and biocides to enzymatic compounds and radiation-based methods. The choice of decontaminant is contingent upon factors such as the type of hazardous material, the contamination level, and the intended decontamination site [12].

• Chemical Decontaminants: Chemical agents, exemplified by oxidizing agents like hydrogen peroxide or chlorine-based compounds, are extensively used in post-decontamination processes. They are prized for their ability to react with and neutralize biological agents and toxins. However, the indiscriminate use of such chemicals can have profound effects on surrounding ecosystems. Runoff from decontamination efforts can contaminate soils and water bodies, leading to adverse ecological consequences [13].

• Biological Agents: Biological decontaminants employ living organisms, such as enzymes or bacteria, to break down or metabolize biorisk materials. While biodegradation is a promising approach, the introduction of non-native organisms into ecosystems may disrupt natural microbial communities, potentially leading to ecological imbalances.

• Radiation-Based Decontamination: Radiation-based methods, including gamma irradiation and electron beam treatment, utilize ionizing radiation to eradicate contaminants. While highly effective, these methods can induce chemical changes in soils and other materials, altering their physicochemical properties and potentially affecting soil fertility and microbial activity [9].

2.2 Environmental Implications

The use of post-decontamination decontaminants, although indispensable for safeguarding human health, engenders a series of environmental implications that demand careful consideration. These implications encompass soil and water contamination, alteration of microbial communities, and disruption of ecosystems [14].

• Soil Contamination: Residues of decontamination agents can persist in soil matrices long after their application, potentially leading to soil pollution. The accumulation of such residues may alter soil chemistry, affecting nutrient availability and soil pH, which, in turn, can influence plant growth and overall ecosystem health.

• Water Contamination: Runoff from decontamination efforts can transport decontaminants into nearby water bodies, raising concerns about water quality. Contaminants can adversely affect aquatic ecosystems, disrupting aquatic life and posing risks to human water resources [15].

• Microbial Community Shifts: The introduction of decontamination agents into soil and water environments can induce shifts in microbial communities. These shifts may favor the development of resistance mechanisms among microorganisms, a phenomenon that can impact ecosystem functioning and resilience.

• Ecosystem Disruption: The cumulative effect of post-decontamination decontaminants on soil, water, and microbial communities can lead to broader ecosystem disruptions. These disruptions may manifest as changes in species composition, habitat degradation, and alterations in trophic dynamics.

Apparently, it becomes evident that post-decontamination decontaminants are not without their ecological consequences. It is imperative to recognize the intricate interplay between human safety and environmental stewardship, seeking a balance that minimizes adverse impacts on ecosystems while ensuring the effective neutralization of biorisk materials [16].

2.3 The Imperative of Post-Decontamination Treatment

The utilization of post-decontamination decontaminants arises from the critical necessity to ensure that residual contamination, often imperceptible to the naked eye, is thoroughly eliminated following initial decontamination procedures [17]. The need for post-decontamination treatment is underscored by several factors:

• Residual Threats: Even the most meticulous initial decontamination processes may leave behind minute traces of biorisk materials. These residual contaminants, although at reduced concentrations, continue to pose a potential threat to human health and the environment. The persistence of such contaminants can result from their adherence to surfaces, penetration into porous materials, or subsurface infiltration into soils [18].

• Persistence of Biological Agents: Biological agents, including microorganisms and their toxins, exhibit tenacity in adverse environmental conditions. Residual spores, for instance, can remain viable for extended periods, posing a latent danger if not effectively neutralized. Consequently, post-decontamination decontaminants are designed to target these lingering threats, preventing their resurgence [19].

• Preventing Recontamination: In scenarios where decontaminated areas are intended for subsequent use, the prevention of recontamination is paramount. Post-decontamination treatment acts as a safeguard against the reintroduction of biorisk materials into spaces where they may pose risks to occupants or the broader environment [20].

• Environmental Resilience: While the focus of post-decontamination treatment is primarily on human safety, it is intrinsically tied to environmental resilience. By ensuring that residual contamination is eliminated, additionally mitigating the potential for ecological perturbations arising from low-level, persistent contamination should be made [21].

In sum, the imperative for post-decontamination treatment lies in its capacity to address residual contamination that lingers in the aftermath of decontamination efforts. This strategic approach safeguards against potential threats, bolsters environmental resilience, and upholds the overarching objective of biorisk material management—namely, the protection of human health and the environment [22].

3 Resistance in Ecosystems: A Growing Concern

In the complex milieu of post-decontamination scenarios, the emergence and proliferation of resistance in ecosystems have become a topic of escalating concern. Resistance, in this context, refers to the ability of microorganisms and other biological entities within ecosystems to withstand and adapt to the presence of post-decontamination decontaminants [23,24].

3.1 The Dynamics of Resistance

Resistance in ecosystems manifests as the capacity of resident organisms to endure and, in some instances, thrive in the presence of post-decontamination decontaminants that were originally intended to eradicate them. These resistant organisms may include bacteria, fungi, algae, or even higher-level organisms within the ecological hierarchy. The dynamics of resistance are shaped by several interrelated factors [25]:

• Selection Pressure: The application of post-decontamination decontaminants exerts a profound selection pressure on microbial populations. Those microorganisms possessing inherent or acquired resistance mechanisms gain a competitive advantage.

• Genetic Adaptation: Resistance can arise through genetic adaptation, involving mutations that confer protection against decontaminants. Genetic changes may occur spontaneously or be transferred horizontally among microbial communities, enabling the rapid dissemination of resistance traits [26].

• Co-Selection: The use of broad-spectrum decontaminants may co-select for resistance to antibiotics or other antimicrobial agents. This phenomenon is particularly concerning in environments where human and veterinary pharmaceuticals coexist with post-decontamination agents.

• Ecological Context: The ecological context plays a pivotal role in resistance dynamics. Environmental conditions, nutrient availability, and the presence of competing or symbiotic species all influence the prevalence and persistence of resistance [27].

3.2 Mechanisms of Resistance

Resistance in ecosystems arises through a spectrum of mechanisms, each conferring a degree of protection against post-decontamination decontaminants. These mechanisms may be intrinsic or acquired, stemming from the acquisition of resistance genes. Key mechanisms include [28]:

• Efflux Pumps: Microorganisms can employ efflux pumps to expel decontaminants from their cellular membranes, reducing their intracellular concentration.

• Enzymatic Degradation: Certain microorganisms produce enzymes capable of degrading decontaminants, rendering them ineffective.

• Biofilm Formation: Microbial communities often encase themselves in protective biofilms, shielding against decontaminant penetration.

• Genetic Resistance Elements: Resistance genes, including those encoding for antibiotic resistance, can be mobilized and disseminated among microorganisms via horizontal gene transfer mechanisms [27].

3.3 Implications of Resistance

Resistance in ecosystems carries significant implications for human health, environmental stability, and biorisk material management:

• Human Health Risks: Resistant microorganisms may persist in the environment, potentially encountering humans or animals. This may raise concerns about the transfer of resistance genes to pathogens, complicating diseases treatment.

• Ecological Resilience: Resistance can alter the composition and functioning of microbial communities, potentially reducing ecosystem resilience and adaptability to environmental changes.

• Long-Term Environmental Impact: The persistence of resistant organisms in the environment may have long-term repercussions, necessitating proactive strategies to mitigate resistance and protect ecosystem health.

The intricate terrain of resistance in ecosystems makes the picture clear that this phenomenon warrants comprehensive examination and proactive management strategies [27,28].

4 Monitoring and Managing Resistance

Effectively addressing resistance in ecosystems necessitates a multifaceted approach that encompasses monitoring, assessment, and adaptive management. This proactive stance is crucial to mitigate the potential consequences of resistance emergence. Several key considerations underpin these efforts [29]:

• Surveillance and Detection: Monitoring the presence and prevalence of resistance in ecosystems is paramount. Molecular techniques, metagenomics, and microbiome analysis offer valuable tools for identifying and quantifying resistance genes and resistant organisms within ecological niches.

• Environmental Risk Assessment: A comprehensive assessment of the environmental risks associated with resistance is indispensable. Such assessments evaluate the potential ecological consequences of resistance, helping to inform management strategies [30].

• Integrated Management: Addressing resistance in ecosystems necessitates an integrated approach that combines ecological restoration, targeted intervention, and responsible decontamination practices. Strategies may include the use of alternative decontamination agents, decontaminant-free zones, and promoting natural attenuation of contaminants.

• Adaptive Management: Given the dynamic nature of resistance and ecosystems, adaptive management strategies are essential. These strategies involve ongoing assessment and adjustment based on evolving data and ecological conditions.

• Drone-Based Monitoring: As technology advances, drones have emerged as powerful tools for real-time monitoring of resistance. Equipped with various sensors, including DNA sequencers and imaging devices, drones can provide valuable data for tracking resistance dynamics in remote or challenging-to-reach environments [31,32].

4.1 Defining Resistance in Ecosystems

Resistance in ecosystems is a multifaceted phenomenon that resonates deeply within the context of post-decontamination scenarios. At its core, resistance denotes the capacity of microorganisms and other biological entities residing within ecosystems to withstand and adapt to the presence of post-decontamination decontaminants, which were originally introduced with the intention of eradicating them. This intricate concept becomes especially pertinent in the wake of decontamination efforts, as it encapsulates the resilience of life forms in the face of chemical, biological, or physical agents designed to curtail their existence. The relevance of resistance in ecosystems emerges from the profound interplay between human interventions, such as decontamination, and the inherent adaptability of organisms to environmental pressures. This adaptability encompasses a spectrum of mechanisms that empower microorganisms and other species to endure the challenges posed by decontaminants. In doing so, these resilient organisms can persist and, in some instances, proliferate, despite the initial intent of rendering them inert [33].

4.2 Decontaminants and the Genesis of Resistance

The use of decontaminants, which constitute an integral component of post-decontamination protocols, may inadvertently precipitate the emergence of resistance in ecosystems. The pathways through which this occurs are complex and multifaceted, reflecting the dynamic nature of microbial communities and ecological systems [34]:

- Selection Pressure: The application of decontaminants creates a potent selection pressure within ecosystems. In essence, it initiates a competitive landscape in which organisms possessing innate or acquired resistance mechanisms gain a distinct advantage. This selection pressure often results from the elimination of susceptible individuals, allowing resistant counterparts to thrive and perpetuate their genetic traits.

- Genetic Adaptation: Resistance can manifest through genetic adaptation, driven by mutations that confer protection against decontaminants. These genetic changes may occur spontaneously within microbial populations or be facilitated by horizontal gene transfer mechanisms, which facilitate the rapid dissemination of resistance traits among microbial communities.

- Co-Selection: Particularly concerning is the phenomenon of co-selection, where the use of decontaminants with broad-spectrum antimicrobial properties inadvertently selects for resistance to other classes of antimicrobial agents, including antibiotics. This co-selection scenario can exacerbate the spread of resistance within ecosystems, compounding the challenge of managing resistant organisms.

- Ecological Dynamics: Resistance dynamics within ecosystems are intricately intertwined with the ecological context. Factors such as environmental conditions, nutrient availability, and the presence of competing or symbiotic species significantly influence the prevalence and persistence of resistance. Consequently, the emergence and propagation of resistance within ecosystems are influenced by a complex web of ecological variables.

Navigating the intricate landscape of resistance in ecosystems, it becomes evident that this phenomenon transcends traditional disciplinary boundaries, necessitating interdisciplinary research and management approaches. A comprehensive understanding of resistance dynamics, their underlying mechanisms, and their ecological consequences is paramount to mitigating the potential risks associated with resistance in the aftermath of decontamination efforts [35,36].

5 The Role of Drones in Resistance Management

The integration of drones into resistance management strategies represents a promising avenue for enhancing our understanding and response to resistance in ecosystems. Drones offer several advantages [37]:

- Real-Time Data Collection: Drones equipped with advanced sensors can collect real-time data on resistance markers, microbial communities, and environmental conditions. This data aids in assessing the extent and dynamics of resistance.

- Remote Sensing: Drones can access remote or hazardous areas, providing valuable insights into resistance in otherwise inaccessible environments, such as post-decontamination sites or contaminated natural reserves.

- Adaptive Sampling: Drones can be programmed to adaptively sample based on detected resistance markers, allowing for targeted sampling and analysis in areas of concern.

- Early Warning Systems: By continuously monitoring resistance markers, drones can serve as early warning systems, alerting stakeholders to emerging resistance trends and facilitating timely intervention.

Resistance in ecosystems represents a multifaceted challenge with far-reaching implications for human health and environmental stability [7]. Grappling with this phenomenon, proactive strategies, including the innovative use of drones, hold promise in enhancing our capacity to detect, monitor, and manage resistance in post-decontamination scenarios.

6 Drones in Environmental Monitoring: Pioneering Precision in Post-Decontamination Assessment

6.1 The Pivotal Role of Drones in Environmental Monitoring

In the realm of post-decontamination assessment and environmental monitoring, the introduction of Unmanned Aerial Vehicles (UAVs), commonly referred to as drones, has marked a transformative paradigm shift. These aerial platforms, equipped with an array of advanced sensors and instrumentation, have emerged as indispensable tools for acquiring real-time data in dynamic and often challenging ecological settings. Their capacity to navigate diverse terrains, access remote or hazardous areas, and capture high-resolution imagery has propelled them to the forefront of environmental monitoring practices [38].

The pivotal role played by drones in environmental monitoring cannot be overstated. Their agility and versatility enable them to execute tasks that were once logistically cumbersome or prohibitively expensive. Moreover, their capacity to collect data in situ, at the heart of environmental processes, affords researchers and environmental managers a level of precision and immediacy previously unattainable. This capacity for real-time data acquisition, paired with their ability to venture into otherwise inaccessible domains, positions drones as instrumental assets in assessing the impact of post-decontamination decontaminants on ecosystems [39].

6.2 Advantages of Drone-Based Assessment in Post-Decontamination Scenarios

The advantages inherent in employing drones to evaluate the impact of post-decontamination decontaminants on ecosystems are manifold and extend across several critical dimensions [8]:

1. Remote Sensing Capabilities: Drones can access remote or challenging terrains, such as contaminated sites or fragile ecosystems, without the need for on-site human presence. This attribute is invaluable in post-decontamination assessments where safety or accessibility may be compromised.

2. Real-Time Data Acquisition: Perhaps their most distinguishing feature, drones provide real-time data, enabling researchers to capture the dynamic nuances of ecological responses immediately after

decontamination efforts. This immediacy is invaluable for assessing the immediate impact of decontaminants.

3. High-Resolution Imaging: Equipped with advanced cameras and imaging systems, drones capture high-resolution imagery, facilitating the precise identification of changes in vegetation, soil conditions, or aquatic ecosystems. This capability enhances the detection of subtle alterations resulting from post-decontamination interventions.

4. Adaptive Sampling: Drones can be programmed to adaptively sample specific areas of concern, focusing data collection efforts where resistance markers, ecological shifts, or contamination hotspots are detected. This targeted approach optimizes resource utilization and data relevance.

5. Improved Safety and Cost-Efficiency: By reducing the need for physical access to hazardous or challenging environments, drones enhance safety for human personnel while minimizing logistical costs associated with extensive fieldwork.

6. Multimodal Sensor Integration: Drones can integrate a diverse range of sensors, including DNA sequencers, spectrometers, and thermal imaging cameras. This multifaceted sensor integration enables comprehensive data collection, allowing for a holistic assessment of environmental changes.

In essence, drones have transcended the realm of technological novelty to become indispensable allies in the pursuit of understanding and mitigating the impact of post-decontamination decontaminants on ecosystems. Their capacity to bridge the gap between human safety and ecological preservation through precise, real-time data acquisition underscores their transformative potential in post-decontamination assessments [40,41]. Figure 1 shows a drone design concept used in post-decontamination.

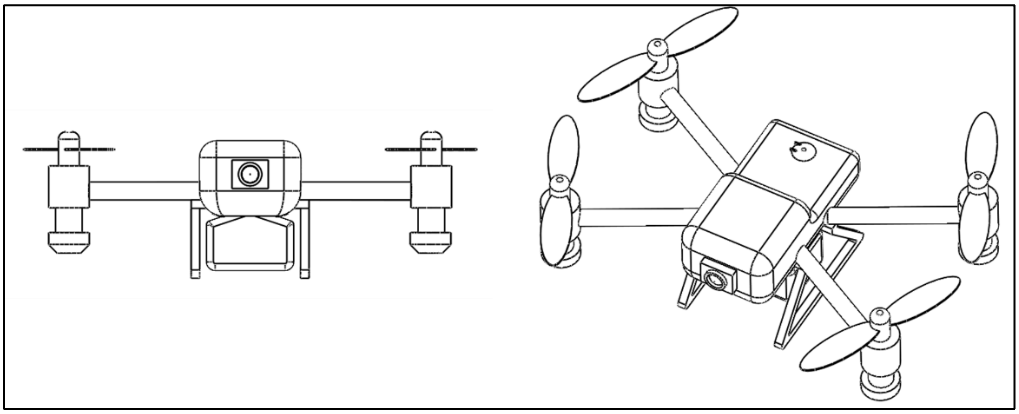

Figure 1: Drone design concept used in post-decontamination.

7 Drone-Based Resistance Detection: Navigating Resistance Frontiers with Precision

7.1 Harnessing Drones for Resistance Detection in Ecosystems

The deployment of drones as instruments of ecological exploration extends beyond their capabilities in environmental monitoring. These aerial platforms have emerged as instrumental allies in the endeavor to detect and scrutinize resistance within ecosystems. The utilization of drones for resistance detection represents an innovative and transformative approach that holds immense promise in our quest to comprehend the complexities of resistance dynamics in the aftermath of decontamination efforts.

Drones, with their real-time data acquisition capacity, can be employed to survey environments for signs of resistance, encompassing changes in microbial populations, genetic adaptations, and shifts in microbial community structures. Their ability to access remote or otherwise challenging ecological niches empowers researchers to venture into areas where resistance may be lurking, providing critical insights into the resilience of ecosystems following decontamination interventions [42,43].

7.2 Sensor Technologies and Data Analysis Methods in Resistance Monitoring

The efficacy of drone-based resistance detection relies heavily on sensor technologies and data analysis methods designed to decipher subtle ecological shifts. Drones can be equipped with an array of sensors tailored to detect resistance markers, assess microbial community dynamics, and capture environmental variables. These sensors may include [44,45]:

- DNA Sequencers: DNA sequencers onboard drones can analyze environmental samples to identify specific resistance genes or mutations. This approach offers unparalleled precision in detecting genetic adaptations linked to resistance [46].

- Spectrometers: Spectrometers enable drones to collect spectral data from ecosystems, revealing changes in vegetation, soil properties, or water quality. Such changes may serve as indirect indicators of resistance-related ecological shifts.

- Thermal Imaging Cameras: Thermal imaging cameras can identify temperature variations in ecosystems, potentially indicating the presence of resistance-associated microbial activity. Elevated temperatures, for instance, may signify the metabolic activity of resistant microorganisms [47].

Data analysis methods in resistance monitoring encompass a spectrum of computational techniques, including bioinformatics, machine learning, and ecological modeling [7]. These methods enable researchers to analyze and interpret the voluminous datasets collected by drones, facilitating the identification of resistance patterns, ecological responses, and correlations with environmental parameters. While exploring the potential of drones for resistance detection, it becomes evident that their integration into resistance monitoring protocols enhances our capacity to discern and understand the intricacies of resistance dynamics within ecosystems [37,48].

8 Remediation Strategies with Drones: Precision in Ecological Restoration

8.1 Drones as Catalysts for Targeted Remediation

Drones, with their capacity for real-time data acquisition and agile maneuverability, extend their transformative influence beyond resistance detection into the realm of targeted ecological remediation. The potential of drones for precision-based interventions in contaminated areas is a testament to their versatility and utility in the preservation of ecosystem health. In contaminated environments, drones can serve as aerial delivery platforms for remediation agents, such as bioremediation microorganisms, enzymes, or specific chemicals [49,50]. By precisely delivering these agents to areas where resistance is detected or contamination persists, drones minimize unnecessary dispersion of remediation resources, thus optimizing their effectiveness. This targeted approach minimizes ecological disruption and maximizes the chances of successful remediation [42,51].

8.2 Case Studies and Drone-Assisted Ecological Restoration

The application of drones in ecological restoration and remediation efforts is exemplified by numerous case studies across various ecosystems. These case studies offer valuable insights into the tangible benefits of drone-assisted restoration [52,53]:

- Riparian Zone Restoration: Drones have been used to reseed native vegetation along riverbanks and wetlands. By dropping seed pods or spraying seeds precisely in areas needing restoration, drones enhance biodiversity and improve habitat quality.
- Contaminated Site Remediation: In contaminated industrial sites, drones have played pivotal roles in the delivery of remediation agents, such as bioremediation microbes or chemical treatments, to specific areas of concern. This approach accelerates the restoration process and minimizes the spread of contaminants.
- Invasive Species Management: Drones have been utilized to identify and manage invasive plant species in sensitive ecosystems. They can disperse herbicides or deploy targeted treatments to control invasive species' spread while minimizing harm to native flora.

These case studies underscore the potential of drones not only as tools for data collection and analysis but also as instruments of ecological healing and rejuvenation. By integrating drones into post-decontamination and restoration protocols, enhancing our ability to address the ecological repercussions of contamination and resistance while fostering ecosystem recovery and resilience [40,54].

9 Integrating Drone Technology: Enabling Adaptive Management

The integration of drone technology into post-decontamination protocols represents a paradigm shift in the realm of biorisk material management. It offers a dynamic approach that aligns human safety with environmental stewardship. By incorporating drones, we bridge the gap between data collection and decision-making, empowering adaptive management strategies that respond to real-time ecological insights. The role of real-time data, facilitated by drones, is central to the concept of adaptive management. Decision-makers are empowered to respond promptly to ecological changes, resistance trends, or unexpected challenges arising from post-decontamination scenarios [40,51]. This agility allows for the dynamic adjustment of remediation strategies, allocation of resources, and implementation of ecological restoration measures. In essence, the integration of drone technology not only enhances our capacity for data collection and ecological understanding but also instills agility and adaptability into the heart of post-decontamination protocols [55,56]. It embodies a holistic approach that recognizes the intricate interplay between human safety, environmental preservation, and the preservation of ecosystem health. As we continue to navigate the evolving landscape of biorisk material management, the role of drones remains pivotal, offering a beacon of hope for the harmonious coexistence of humanity and nature in an era of increasing technological advancement [57,58].

10 Conclusion: Forging a Sustainable Path Forward

The confluence of post-decontamination decontaminants, resistance in ecosystems, and the transformative potential of drones has illuminated the intricate terrain of biorisk material management and environmental stewardship. In our pursuit of a sustainable path forward, several key takeaways emerge:

1. Environmental Guardianship: Biorisk material management extends beyond human safety; it embodies our responsibility as environmental stewards. Recognizing the potential ecological

consequences of decontaminants and the emergence of resistance underscores the urgency of harmonizing human interests with those of the environment.

2. Precision and Agility: Drones epitomize precision and agility in post-decontamination scenarios. Their real-time data acquisition capacity empowers us to make informed, adaptive decisions that mitigate ecological harm and promote resilience.

3. Interdisciplinary Collaboration: Effective management of resistance and environmental consequences requires interdisciplinary collaboration. Experts from fields spanning microbiology, ecology, technology, and policy must collaborate to navigate this complex landscape.

4. Innovation and Adaptation: The evolving landscape of biorisk material management demands innovation and adaptation. The integration of drones exemplifies our capacity to harness cutting-edge technology for the greater good of humanity and the environment.

5. Holistic Perspective: A holistic perspective, one that encompasses human safety, environmental health, and ecological resilience, is paramount. As we advance in our understanding of resistance and environmental dynamics, this perspective guides our decision-making.

In our collective journey through the realms of decontamination, resistance, and the innovative application of drone technology, we have unraveled the profound interconnectedness of human endeavors with the delicate ecosystems that cradle our existence. The path forward is illuminated by a stark yet compelling realization: we bear a shared imperative to safeguard our world. At the intersection of science, technology, and environmental stewardship, we find the blueprint for a sustainable future. Our responsibility extends beyond the preservation of human safety; it encompasses the protection of the intricate web of life that thrives alongside us. Resistance in ecosystems, often sparked by the very interventions intended to protect us, underscores the need for vigilance and ecological mindfulness.

The role of drones, as our emissaries into the unknown, symbolizes our unwavering commitment to harmonize the interests of humanity with those of the environment. Their ability to collect real-time data, pinpoint resistance, facilitate restoration, and guide adaptive management signifies a transformative force that we must embrace and wield responsibly. As we conclude this exploration, let us not forget the imperative to save the world—one ecosystem, one habitat, one species at a time. The world we share is an irreplaceable tapestry of life, intricately woven by the forces of evolution, time, and nature's wisdom. It is our privilege and duty to act as its guardians, ensuring that the delicate threads of biodiversity remain unbroken, the ecosystems resilient, and the planet habitable for generations to come. In the face of evolving challenges and advancing science, let us remain steadfast in our commitment to protect, preserve, and prosper together. The fate of our world is intertwined with our choices, and it is within our power to chart a course towards a sustainable, harmonious coexistence—one that saves not only ourselves but the remarkable world we call home.

11 Declarations

11.1 Acknowledgements

Authors have conflict of interest to declare. We would like to thank Fatma ALTINTAŞ for her kind interest in our study.

11.2 Authors' Contributions

Ahmet Koluman: Wrote the paper, build the concept and made the research.

Atakan Konukbay: Designed the concept, added the CBRN approaches, edited the language and corrected the proof.

References

[1] Yates, S. R., McConnell, L. L., Hapeman, C. J., Papiernik, S. K., Gao, S., & Trabue, S. L. (2011). Managing agricultural emissions to the atmosphere: state of the science, fate and mitigation, and identifying research gaps. Journal of Environmental Quality, 40(5), 1347-1358.

[2] Covello, V. T., & Frey, R. S. (1990). Technology-based environmental health risks in developing nations. Technological Forecasting and Social Change, 37(2), 159-179.

[3] DiEuliis, D., & Giordano, J. (2018). Gene editing using CRISPR/Cas9: implications for dual-use and biosecurity. Protein & Cell, 9(3), 239-240.

[4] Ormerod, S. J. (2003). Restoration in applied ecology: editor's introduction. Journal of applied ecology, 40(1), 44-50.

[5] de Almeida, D. R. A., Almeyda Zambrano, A. M., Broadbent, E. N., Wendt, A. L., Foster, P., Wilkinson, B. E., ... & Chazdon, R. (2020). Detecting successional changes in tropical forest structure using GatorEye drone-borne lidar. Biotropica, 52(6), 1155-1167.

[6] Poljak, M., & Šterbenc, A. J. C. M. (2020). Use of drones in clinical microbiology and infectious diseases: current status, challenges and barriers. Clinical Microbiology and Infection, 26(4), 425-430.

[7] Corcoran, E., Winsen, M., Sudholz, A., & Hamilton, G. (2021). Automated detection of wildlife using drones: Synthesis, opportunities and constraints. Methods in Ecology and Evolution, 12(6), 1103-1114.

[8] Kitonsa, H., & Kruglikov, S. V. (2018). Significance of drone technology for achievement of the United Nations sustainable development goals. R-economy, 4(3), 115-120.

[9] Magalhães, S. M. C., Jorge, R. F., & Castro, P. M. (2009). Investigations into the application of a combination of bioventing and biotrickling filter technologies for soil decontamination processes—a transition regime between bioventing and soil vapour extraction. Journal of hazardous materials, 170(2-3), 711-715.

[10] Adebiyi, F. M., Ore, O. T., Adeola, A. O., Durodola, S. S., Akeremale, O. F., Olubodun, K. O., & Akeremale, O. K. (2021). Occurrence and remediation of naturally occurring radioactive materials in Nigeria: a review. Environmental Chemistry Letters, 19, 3243-3262.

[11] Yair, S., Ofer, B., Arik, E., Shai, S., Yossi, R., Tzvika, D., & Amir, K. (2008). Organophosphate degrading microorganisms and enzymes as biocatalysts in environmental and personal decontamination applications. Critical reviews in biotechnology, 28(4), 265-275.

[12] Bi, J., Tao, Q., Huang, X., Wang, J., Wang, T., & Hao, H. (2021). Simultaneous decontamination of multi-pollutants: A promising approach for water remediation. Chemosphere, 284, 131270.

[13] Bernardo, M., Gonçalves, M., Lapa, N., Barbosa, R., Mendes, B., & Pinto, F. (2012). Characterization of chars produced in the co-pyrolysis of different wastes: Decontamination study. Journal of hazardous materials, 207, 28-35.

[14] Quaranta, G., Vincenti, S., Ferriero, A. M., Boninti, F., Sezzatini, R., Turnaturi, C., ... & Laurenti, P. (2012). Legionella on board trains: effectiveness of environmental surveillance and decontamination. BMC Public Health, 12(1), 1-7.

[15] VAN SAENE, H. K., STOUTENBEEK, C. C., & STOLLER, J. K. (1992). Selective decontamination of the digestive tract in the intensive care unit: current status and future prospects. Critical care medicine, 20(5), 691-703.

[16] Gurtler, J. B. (2017). Pathogen decontamination of food crop soil: a review. Journal of Food Protection, 80(9), 1461-1470.

[17] Stingl, K., Knüver, M. T., Vogt, P., Buhler, C., Krüger, N. J., Alt, K., ... & Käsbohrer, A. (2012). Quo vadis?—monitoring Campylobacter in Germany. European Journal of Microbiology and Immunology, 2(1), 88-96.

[18] Chilcott, R. P., Larner, J., Durrant, A., Hughes, P., Mahalingam, D., Rivers, S., ... & Reppucci, J. (2019). Evaluation of US Federal Guidelines (Primary Response Incident Scene Management [PRISM]) for mass decontamination of casualties during the initial operational response to a chemical incident. Annals of emergency medicine, 73(6), 671-684.

[19] Kang, L., Mermel, L. A., & Trafton, P. G. (2008). What happens when autogenous bone drops out of the sterile field during orthopaedic trauma surgery. Journal of orthopaedic trauma, 22(6), 430-431.

[20] Carter, H., Weston, D., Betts, N., Wilkinson, S., & Amlôt, R. (2018). Public perceptions of emergency decontamination: Effects of intervention type and responder management strategy during a focus group study. PloS one, 13(4), e0195922.

[21] Yasutaka, T., Naito, W., & Nakanishi, J. (2013). Cost and effectiveness of decontamination strategies in radiation contaminated areas in Fukushima in regard to external radiation dose. PloS one, 8(9), e75308.

[22] Love, A. H., Bailey, C. G., Hanna, M. L., Hok, S., Vu, A. K., Reutter, D. J., & Raber, E. (2011). Efficacy of liquid and foam decontamination technologies for chemical warfare agents on indoor surfaces. Journal of hazardous materials, 196, 115-122.

[23] Litvak, Y., & Bäumler, A. J. (2019). The founder hypothesis: a basis for microbiota resistance, diversity in taxa carriage, and colonization resistance against pathogens. PLoS pathogens, 15(2), e1007563.

[24] Camiade, M., Bodilis, J., Chaftar, N., Riah-Anglet, W., Gardères, J., Buquet, S., ... & Pawlak, B. (2020). Antibiotic resistance patterns of Pseudomonas spp. isolated from faecal wastes in the environment and contaminated surface water. FEMS microbiology ecology, 96(2), fiaa008.

[25] Yang, L., Barnard, R., Kuzyakov, Y., & Tian, J. (2021). Bacterial communities drive the resistance of soil multifunctionality to land-use change in karst soils. European journal of soil biology, 104, 103313.

[26] Álvarez-Martínez, F. J., Barrajón-Catalán, E., & Micol, V. (2020). Tackling antibiotic resistance with compounds of natural origin: A comprehensive review. Biomedicines, 8(10), 405.

[27] Koluman, A., & Dikici, A. (2013). Antimicrobial resistance of emerging foodborne pathogens: status quo and global trends. Critical reviews in microbiology, 39(1), 57-69.

[28] Koluman, A., Dikici, A., Kahraman, T., & Ncili, G. K. (2017). Food safety and climate change: seasonality and emerging foodborne pathogens. Journal of Gastroenterology Research, 1(1), 24-29.

[29] Nunez-Mir, G. C., Liebhold, A. M., Guo, Q., Brockerhoff, E. G., Jo, I., Ordonez, K., & Fei, S. (2017). Biotic resistance to exotic invasions: its role in forest ecosystems, confounding artifacts, and future directions. Biological Invasions, 19, 3287-3299.

[30] Daglish, G. J., Nayak, M. K., & Pavic, H. (2014). Phosphine resistance in Sitophilus oryzae (L.) from eastern Australia: Inheritance, fitness and prevalence. Journal of Stored Products Research, 59, 237-244.

[31] Hoffmann, A. A., Hallas, R. J., Dean, J. A., & Schiffer, M. (2003). Low potential for climatic stress adaptation in a rainforest Drosophila species. Science, 301(5629), 100-102.

[32] Beier, C. M., Patterson, T. M., & Chapin, F. S. (2008). Ecosystem services and emergent vulnerability in managed ecosystems: a geospatial decision-support tool. Ecosystems, 11, 923-938.

[33] Downing, A. S., van Nes, E. H., Mooij, W. M., & Scheffer, M. (2012). The resilience and resistance of an ecosystem to a collapse of diversity.

[34] Fritz, M. L., Hamby, K. A., Taylor, K., DeYonke, A. M., & Gould, F. (2020). Genome evolution in an agricultural pest following adoption of transgenic crops. bioRxiv, 2020-10.

[35] Chambers, J. C., Brooks, M. L., Germino, M. J., Maestas, J. D., Board, D. I., Jones, M. O., & Allred, B. W. (2019). Operationalizing resilience and resistance concepts to address invasive grass-fire cycles. Frontiers in Ecology and Evolution, 7, 185.

[36] Birgé, H. E., Allen, C. R., Garmestani, A. S., & Pope, K. L. (2016). Adaptive management for ecosystem services. Journal of Environmental Management, 183, 343-352.

[37] James, K., & Bradshaw, K. (2020). Detecting plant species in the field with deep learning and drone technology. Methods in Ecology and Evolution, 11(11), 1509-1519.

[38] Zhang, J., Hu, J., Lian, J., Fan, Z., Ouyang, X., & Ye, W. (2016). Seeing the forest from drones: Testing the potential of lightweight drones as a tool for long-term forest monitoring. Biological Conservation, 198, 60-69.

[39] Simic Milas, A., Sousa, J. J., Warner, T. A., Teodoro, A. C., Peres, E., Gonçalves, J. A., ... & Woodget, A. (2018). Unmanned Aerial Systems (UAS) for environmental applications special issue preface. International Journal of Remote Sensing, 39(15-16), 4845-4851.

[40] Robinson, J. M., Harrison, P. A., Mavoa, S., & Breed, M. F. (2022). Existing and emerging uses of drones in restoration ecology. Methods in Ecology and Evolution, 13(9), 1899-1911.

[41] Alsamhi, S. H., Ma, O., Ansari, M. S., & Gupta, S. K. (2019). Collaboration of drone and internet of public safety things in smart cities: An overview of qos and network performance optimization. Drones, 3(1), 13.

[42] Ancin-Murguzur, F. J., Munoz, L., Monz, C., & Hausner, V. H. (2020). Drones as a tool to monitor human impacts and vegetation changes in parks and protected areas. Remote Sensing in Ecology and Conservation, 6(1), 105-113.

[43] Cruzan, M. B., Weinstein, B. G., Grasty, M. R., Kohrn, B. F., Hendrickson, E. C., Arredondo, T. M., & Thompson, P. G. (2016). Small unmanned aerial vehicles (micro-UAVs, drones) in plant ecology. Applications in plant sciences, 4(9), 1600041.

[44] Paneque-Gálvez, J., McCall, M. K., Napoletano, B. M., Wich, S. A., & Koh, L. P. (2014). Small drones for community-based forest monitoring: An assessment of their feasibility and potential in tropical areas. Forests, 5(6), 1481-1507.

[45] Rahman, D. A., Sitorus, A. B. Y., & Condro, A. A. (2021). From Coastal to Montane Forest Ecosystems, Using Drones for Multi-Species Research in the Tropics. Drones, 6(1), 6.

[46] Assmann, J. J., Myers-Smith, I. H., Kerby, J. T., Cunliffe, A. M., & Daskalova, G. N. (2020). Drone data reveal heterogeneity in tundra greenness and phenology not captured by satellites. Environmental Research Letters, 15(12), 125002.

[47] Barreto, J., Cajaiba, L., Teixeira, J. B., Nascimento, L., Giacomo, A., Barcelos, N., ... & Martins, A. (2021). Drone-monitoring: Improving the detectability of threatened marine megafauna. Drones, 5(1), 14.

[48] Brunton, E. A., Leon, J. X., & Burnett, S. E. (2020). Evaluating the efficacy and optimal deployment of thermal infrared and true-colour imaging when using drones for monitoring kangaroos. Drones, 4(2), 20.

[49] Jiménez López, J., & Mulero-Pázmány, M. (2019). Drones for conservation in protected areas: Present and future. Drones, 3(1), 10.

[50] Bloom, D., Butcher, P. A., Colefax, A. P., Provost, E. J., Cullis, B. R., & Kelaher, B. P. (2019). Drones detect illegal and derelict crab traps in a shallow water estuary. Fisheries Management and Ecology, 26(4), 311-318.

[51] Euchi, J. (2021). Do drones have a realistic place in a pandemic fight for delivering medical supplies in healthcare systems problems?. Chinese Journal of Aeronautics, 34(2), 182-190.

[52] Kelaher, B. P., Colefax, A. P., Tagliafico, A., Bishop, M. J., Giles, A., & Butcher, P. A. (2019). Assessing variation in assemblages of large marine fauna off ocean beaches using drones. Marine and Freshwater Research, 71(1), 68-77.

[53] Benayas, J. M. R., Newton, A. C., Diaz, A., & Bullock, J. M. (2009). Enhancement of biodiversity and ecosystem services by ecological restoration: a meta-analysis. science, 325(5944), 1121-1124.

[54] Kollmann, J., Meyer, S. T., Bateman, R., Conradi, T., Gossner, M. M., de Souza Mendonça Jr, M., ... & Weisser, W. W. (2016). Integrating ecosystem functions into restoration ecology—recent advances and future directions. Restoration Ecology, 24(6), 722-730.

[55] Restás, Á. (2022). Drone applications fighting COVID-19 pandemic—Towards good practices. Drones, 6(1), 15.

[56] Franco, C., & Bouri, N. (2010). Environmental decontamination following a large-scale bioterrorism attack: federal progress and remaining gaps. Biosecurity and Bioterrorism: Biodefense Strategy, Practice, and Science, 8(2), 107-117.

[57] Restás, Á., Szalkai, I., & Óvári, G. (2021). Drone application for spraying disinfection liquid fighting against the covid-19 pandemic—examining drone-related parameters influencing effectiveness. Drones, 5(3), 58.

[58] Kunovjanek, M., & Wankmüller, C. (2021). Containing the COVID-19 pandemic with drones-Feasibility of a drone enabled back-up transport system. Transport Policy, 106, 141-152.

Research Paper
Journal of Smart Systems Research (JOINSSR) 5(1),17-32,2024
Received: 30-November-2023 Accepted: 29-January-2024
DOI: 10.58769/joinssr.1398068

SAKARYA UNIVERSITY OF APPLIED SCIENCES

Geniş Bantlı Yüksek Performanslı Antipodal Vivaldi Anteni: Kablosuz İletişim Sistemleri için Verimli Bir Tasarım

Mehmet DUMAN*[1], Volkan BERK[2]

[1] Elektrik Elektronik Mühendisliği Bölümü, Mühendislik Fakültesi, Düzce Üniversitesi, Türkiye.
mehmetduman@duzce.edu.tr mehmetduman@ieee.org
[2] Elektrik Elektronik Mühendisliği Bölümü, Teknoloji Fakültesi, Düzce Üniversitesi, Türkiye.
volkanberkpa@gmail.com

ÖZ

Bu çalışma, CST Studio bilgisayar programı ve bu programın optimize yöntemlerini kullanarak; imal edilen antipodal Vivaldi anteninin, FR-4 dielektrik alt-taban malzemesi yüzeylerine baskı devre aşamalarını; akabinde vektör ağ analizörü cihazında yapılan ölçümleri kapsar. Temel gaye, antenin çeşitli mobil haberleşme teknolojileriyle uyumlu bir şekilde çalışabilmesi için, istenen frekanslarda, en iyileme işlemi uygulanmasıyla elde edilen antenin tasarım ve üretim süreçlerini geliştirmektir. En iyileme işlemi için genetik algoritma, parçacık sürü algoritması ve parametrik tarama algoritması olmak üzere üç farklı yöntem kullanılmıştır. Her bir optimizasyon yönteminden sonra CST Studio programı tarafından zaman alanında üretilen benzetim grafikleri yorum yapılarak paylaşılmıştır. Teorik hesaplamalar, tasarım, benzetim, optimizasyon ve üretim süreçlerinden sonra gerçek test ortamındaki deneylerde VNA cihazı tarafından ölçülen grafikler bilgisayar programı vasıtasıyla varılan grafiklerle karşılaştırılmıştır. Laboratuvar analizlerine göre ilk ölçümler, tasarımı ve üretimi yapılan antipodal Vivaldi anteninin sırasıyla 807 MHz, 2643 MHz ve 3050 MHz frekanslarında başarıyla çalıştığını göstermektedir. Merkez frekanslar olarak kullanılabilecek bu frekansların S11 saçılma değerlerini en düşük olarak verdiği tespit edilmiştir. Laboratuvar ölçümünde elde edilen 2,64 GHz merkez frekansı için bant genişliği -17,719 dB'nin 3 dB fazlası olan -14,719 dB verisinin ölçüldüğü sol ve sağ aralıklar arası olan 2,53 GHz ve 2,77 GHz frekansları arası olup bant genişliği yaklaşık 240 MHz'dir. Aynı şekilde, diğer merkez frekansların bant genişliği de hesaba katılırsa; tüm bu veriler, antenin farklı iletişim teknikleriyle uyumluca kullanılabileceğini ve geniş spektrum uyumluluğuna sahip olduğunu göstermektedir. Sonuç olarak, en iyileme süreci geçiren antipodal Vivaldi antene ait bilgiler, endüstriyel uygulamalar ve yeni akademik çalışmalar için değerli referanslar sunarak gelecekteki kablosuz iletişim teknolojilerinin gelişimine katkı sağlayabilecek niteliktedir.

Anahtar Kelimeler: Antipodal Vivaldi anten, geniş bant iletişim, kablosuz haberleşme sistemleri.

* Sorumlu yazarın e-posta adresi: mehmetduman@duzce.edu.tr

Broadband High-Performance Antipodal Vivaldi Antenna: An Efficient Design for Wireless Communication Systems

ABSTRACT

This study covers the printed circuit stages on the surfaces of FR-4 dielectric substrate materials of the manufactured antipodal Vivaldi antenna using the CST Studio computer program and its optimization methods. Subsequently, measurements conducted on a vector network analyzer device are included. The primary objective is to improve the design and production processes of the antenna obtained through the application of optimization processes at the desired frequencies for the antenna to work compatibly with various mobile communication technologies. Three different methods, namely genetic algorithm, particle swarm algorithm, and parametric scanning algorithm, are used for the optimization process. Simulation graphics generated in the time domain by the CST Studio program after each optimization method are interpreted and shared. Theoretical calculations, design, simulation, optimization, and production processes are compared with the graphs reached through the computer program in experiments in the real test environment by the VNA device. According to laboratory analyses, initial measurements show that the designed and manufactured antipodal Vivaldi antenna successfully operates at frequencies of 807 MHz, 2643 MHz, and 3050 MHz, respectively. It is determined that these frequencies, which can be used as center frequencies, provide the lowest S11 scattering values. The bandwidth for the 2.64 GHz center frequency obtained in laboratory measurements is approximately 240 MHz, with frequencies between 2.53 GHz and 2.77 GHz where the -14.719 dB data, 3 dB beyond -17.719 dB, is measured. Similarly, considering the bandwidth of other center frequencies, all these data indicate that the antenna can be used compatibly with different communication techniques and has wide spectrum compatibility. In conclusion, the information related to the antipodal Vivaldi antenna undergoing the optimization process provides valuable references for industrial applications and new academic studies, contributing to the development of future wireless communication technologies.

Keywords: Antipodal Vivaldi antenna, broadband communications, wireless communication systems.

1 Giriş

Mikrodalga antenler, kablosuz iletişim sistemlerinin temel bileşenleri olarak büyük bir öneme sahiptirler. Kablosuz iletişim teknolojilerindeki hızlı gelişmeler, yüksek veri hızlarına ve geniş kanal kapasitesine ihtiyaç duyulmasına neden olduğundan verimli bir geniş bant antene olan ihtiyaç artmıştır [1]. Antipodal Vivaldi anteni yeterli bant genişliğine sahip olmak, yönlülüğü korumak ve verimliliği artırmak gibi zorlukların üstesinden gelmek için uygun bir çözüm sunar [2]. Tasarım ilkeleri, geniş bant spektrumu elde etmek için farklı bir yapının kullanılmasını içerir.

Antipodal Vivaldi anten ile ilgili son yıllarda birçok çalışma yapılmıştır. M. Wang çalışmasında karaciğer mikrodalga termal ablasyonunu izlemek için bir görüntüleme sistemi tasarımı sunmuştur. Bu sistemin bir parçası olarak, kompakt bir yuva yüklü antipodal Vivaldi anten kullanılmaktadır [3]. S. Kumar 5G iletişimi için yüksek verimli, geniş bant genişliğine sahip ve güçlü iletim performansı sağlayan çift bant antipodal Vivaldi anten dizaynını ele alan bir çalışma gerçekleştirmiştir [4]. J. Wang uzak alanda ultra geniş bant sinyal tespiti için gelişmiş hassasiyet ve doğruluk sağlama amacı güden bir antipodal vivaldi anten tasarımı gerçekleştirmiştir [5]. Antipodal Vivaldi anten (diğer bir adı Tapered Slot Antenna (TSA)), geniş bant genişliği ve yüksek yönlülük özellikleri nedeniyle çeşitli uygulamalarda tercih edilen bir tasarımdır [6]. Gerçekleştirilen tüm bu çalışmaların ortak noktaları olarak antipodal Vivaldi antenlerin geniş bant iletime sahip olması, boyutlarının kuçük olabilmesi, doğru yönlendirebilme kabiliyetleri sıralanabilir. İlgili çalışmalarla birlikte antipodal Vivaldi antenin, mikrodalga frekans bandındaki iletişim sistemlerinin performansını artırmak ve tasarım zorluklarının üstesinden gelmek için önemli bir potansiyele sahip olduğu görülmektedir.

Bu çalışma, antipodal Vivaldi anten odaklı olup FR-4 dielektrik alt-tabanı kullanılarak 800 MHz ve 2,6 GHz merkez frekanslarındaki uygulamalarda çalışabilecek bir çift-bant (dual-band) anten tasarımı oluşturmayı ve optimizasyon araçlarıyla beraber anten tasarım parametrelerinin anten performansına olan etkisini incelemeyi amaçlamaktadır. Antipodal Vivaldi antenin performansı benzetim ve deneysel tabanlı bir yaklaşım benimsenerek analiz edilmiştir. Benzetim kısmında anten tasarımının iyileştirilmesi için üç farklı yöntem kullanılmıştır. Bunlar sırasıyla “Genetic” (Genetik) algoritması, “Particle Swarm” (Parçacık Sürüsü) algoritması ve “Parameter Sweep” (Parametrik Tarama) optimizasyonlarıdır. Bu yöntemler sayesinde antenin tasarım parametreleri istenilen çalışma bölgesine göre optimum sonucu göstererek ortaya çıkmaktadır. Bu çalışmanın kablosuz haberleşme sistemleri için daha etkin ve verimli anten tasarımlarının geliştirilmesine katkı sağlaması beklenmektedir.

2 Metodoloji

Kablosuz haberleşme sistemlerinden telefon iletişimi, WiFi, WiMAX gibi uygulamalarda kullanılabilecek olan nihai antenin sorunsuz çalışabilmesi için çeşitli parametrik taramalardan geçirilerek en iyinin elde edilmesi çalışmanın ana hedefidir. 2G, 3G, 4G, 4,5G ve 5G kablosuz iletişim standartlarına uyan bir tasarım gerçekleştirmek çalışmanın kapsamı içerisindedir. Türkiye için 2G bağlantısı 900 MHz ve 1800 MHz civarlarında, 4,5G bağlantısı 800 MHz, 1800 MHz, 2100 MHz ve 2600 MHz frekansı çevrelerinde olurken; İspanya baz alındığında 2G bağlantılar için 900 MHz ve 1800 MHz, 3G bağlantıları için 900 MHz ve 2100 MHz, 4G bağlantıları için 800 MHz, 1800 MHz ve 2600 MHz, 5G bağlantılar için ise 700 MHz ve 3500 MHz frekanslarında bahsedilen haberleşmeler gerçekleşmektedir. Kullanılması planlanan antenlerin girişten geri yansıma parametresinin (S11) -10 dB ve altındaki değerlerde olması beklenmektedir [7]. Eğer S11, güç, verimlilik gibi faktörler yeterli seviyede olursa üretilecek olan anten ülkeden ülkeye farklı kullanım alanlarına sahip olabilir.

100 – 900 MHz aralığında çalışmaya el verişli olması sebebiyle, Şekil 1’deki Vivaldi anten tasarımı tercih edilerek yeni bir tasarım sürecine girilmiştir, Şekil 1’deki her bir uzunluğun anten ışımasına etkisi vardır [8]. CST programında çizilip isterleri oluşturulduktan sonra FR-4 dielektrik alt-tabana baskısı yapılacaktır.

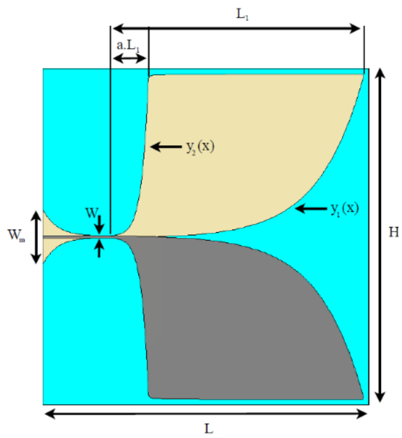

Şekil 1. Esneyebilen Vivaldi anten tasarımı [8]

2.1 Tasarım Süreci

Anten tasarımının bilgisayar ortamında oluşturulması ve benzetiminin gerçekleştirilmesi için CST Studio Suite programı kullanılmıştır. CST Studio Suite, elektromanyetik alan simülasyonu ve analizi için kullanılan kapsamlı bir yazılım paketidir. Tasarımda kullanılan parametler Tablo 1'de görülebilir. Tasarıma ait görsel Şekil 2'de yer almaktadır.

Tablo 1. *Tasarım Parametreleri*

Sembol	Açıklama	Değişken	Birim
Uzunluk	Alt-taban Uzunluk	130	mm
Genişlik	Alt-taban Genişlik	130	mm
a	En uzak nokta çarpanı	0,7	-
b	En kısa nokta çarpanı	0,01	-
G_1	a × Genişlik	91	mm
G_2	b × Genişlik	0,91	mm
TK	Alt-taban Kalınlık	1,5	mm
N_1	Üst yüzey en yakın nokta	0,0927682426293416	mm
N_2	Üst yüzey en uzak nokta	9,14040238101027	mm
N_{-1}	Alt yüzey en yakın nokta	0,0921134159581726	mm
N_{-2}	Alt yüzey en uzak nokta	9,07062502207712	mm
U_{mikro}	Mikroşerit kalınlığı	4	mm
U_{gnd}	Toprak yüzeyi kenar uzunluğu	L/4 = 32,5	mm

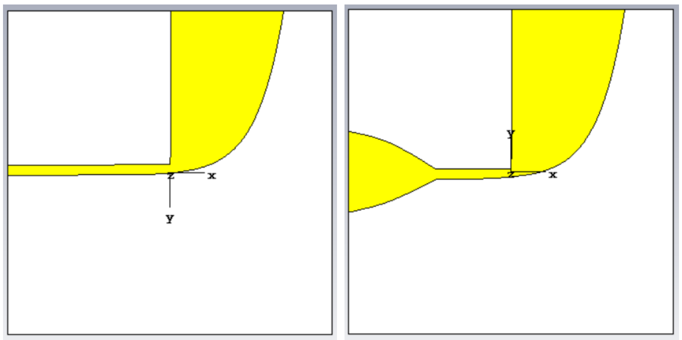

(a) (b)

Şekil 2. Antipodal Vivaldi anten tasarımı

Şekil 2 (a)'da antenin ön yüzeyi, Şekil 2 (b)'de antenin arka yüzeyi yer almaktadır. Arka yüzey toprak yüzeyi olarak kullanılırken, ön yüzey canlı uç teması ile tasarlanmıştır. Tasarımda sarı renkteki alan bakır yüzeyi gösterirken beyaz renkteki alan ise FR-4 içindeki dielektrik malzemeye ait alanı göstermektedir.

2.1.1 Hesaplama

Şekil 1'de yer alan tasarımda $y_1(x)$ ve $y_2(x)$ fonksiyonları birer üstel fonksiyondur ve denklemleri:

$$y_{u1}(x) = e^{N_1 x} - \frac{U_{mikro}}{2} - 1 \tag{1}$$

$$y_{u2}(x) = e^{N_2 x} + \frac{U_{mikro}}{2} - 1 \tag{2}$$

$$N_{u1} = k_{u1} * \ln\left(\frac{Uzunluk + U_{mikro}}{2} + 1\right) \; [k_{u1} = (G_1)^{-1}] \tag{3}$$

$$N_{u2} = k_{u2} * \ln\left(\frac{Uzunluk - U_{mikro}}{2} + 1\right) \; [k_{u2} = (G_2)^{-1}] \tag{4}$$

olarak yazılabilir. Bu denklemler üst tabanı oluşturan denklemlerdir. Alt taban için kullanılan formül:

$$y_{a1}(x) = -e^{N_1 x} + \frac{U_{mikro}}{2} + 1 \tag{5}$$

$$y_{a2}(x) = -e^{N_2 x} - \frac{U_{mikro}}{2} + 1 \tag{6}$$

$$N_{a1} = k_{a1} * \ln\left(\frac{Uzunluk}{2} + \frac{U_{mikro}}{2} + 1\right) \; [k_{a1} = {G_1}^{-1}] \tag{7}$$

$$N_{a2} = k_{a2} * \ln\left(\frac{Uzunluk}{2} - \frac{U_{mikro}}{2} + 1\right) \; [k_{a2} = {G_2}^{-1}] \tag{8}$$

denklemleri ile aktarılabilir.

2.2 Benzetim Süreci

Simülasyon süreci için mikroşerit anten uygulamalarında yapılan adımlar izlendi. Bu adımların başında port yerleştirilecek olan yüzeyin seçilmesi gelmektedir. Şekil 3'te olduğu gibi port için yüzey seçilmesi ile beraber port büyüklüğünün hesaplanması gerekir. Program üzerinde "Macros" sekmesinden seçilen yüzey için "Calculate Port Extension Coefficient (Port Uzatma Katsayısını Hesapla)" işlemi gerçekleştirilebilir. Böylece program, yüzey için gerekli olan port ayarlarını gerçekleştirmiş olur.

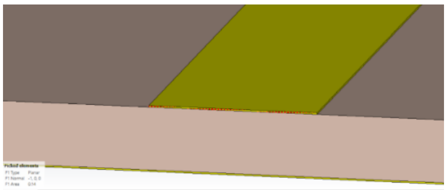

Şekil 3. Port için seçilen yüzey

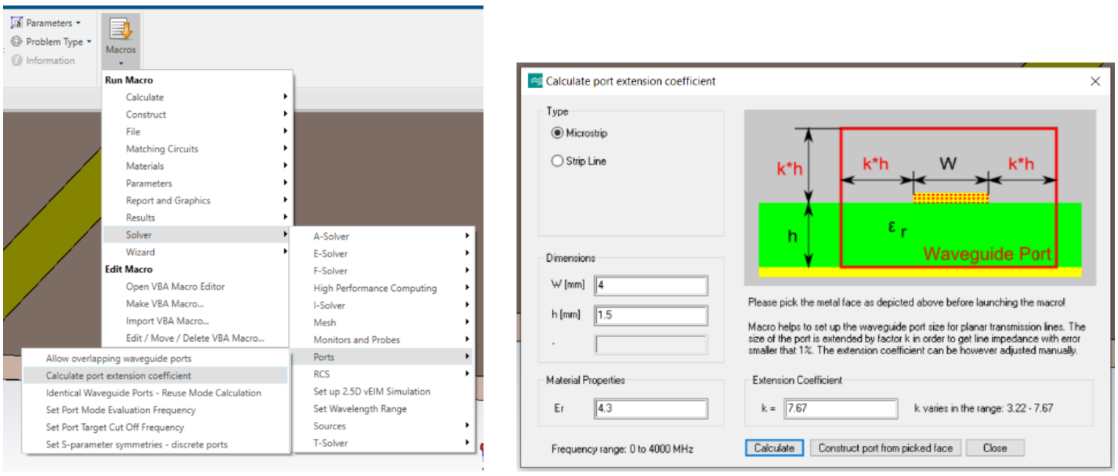

(a) (b)

Şekil 4. Port hesaplamaları

Şekil 4'te görüleceği üzere mikroşerit yüzeyi (W) 4 mm, alt-taban kalınlığı 1,5 mm, program üzerinden hesaplanan katsayı değeri (k) 7,67 bulunmuştur. Şekil 4 (b)'de yer alan "Construct port from picked face (Seçilen yüzey üzerinde port oluştur)" butonuna basılması ile birlikte Şekil 5'te yer alan port oluşturulmuş olur. Portun ayarlanması ile birlikte simülasyon işlemi başlatılır ve antenin karakteristiğine ait bulgular elde edilir.

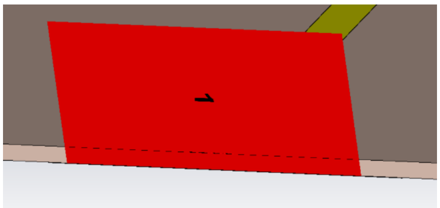

Şekil 5. Portun ayarlanması

2.3 Optimizasyon Süreci

2.3.1 Genetik Algoritma

Bu çalışmada optimizasyon için 3 yöntem kullanılacağı belirtilmişti. Bunlardan ilki genetik Algoritma'dır. Genetik Algoritma (GA), ilk olarak 1960'larda Michigan Üniversitesi'nden John Holland tarafından tanıtılan çokça kullanılan bir doğal sezgisel algoritmadır. Algoritma, biyolojik kalıtım ve doğadaki evrim ilkelerine dayanmaktadır [9].

Genetik algoritma; bir problemin çözümünü, her kromozomun bir çözümü temsil ettiği farklı kromozomlara kodlayarak çalışır. Her bireyin uygunluğu değerlendirilir ve daha yüksek çaprazlama ve mutasyon olasılığı ile bir sonraki nesil için seçilir. Seçilen son birey, problemin en uygun çözümüdür [10]. CST programında genetik algoritmanın ayarlanması gereken birkaç parametre bulunmaktadır. Bu parametre ayarlarıyla ilgili görsel Şekil 6'daki gibidir:

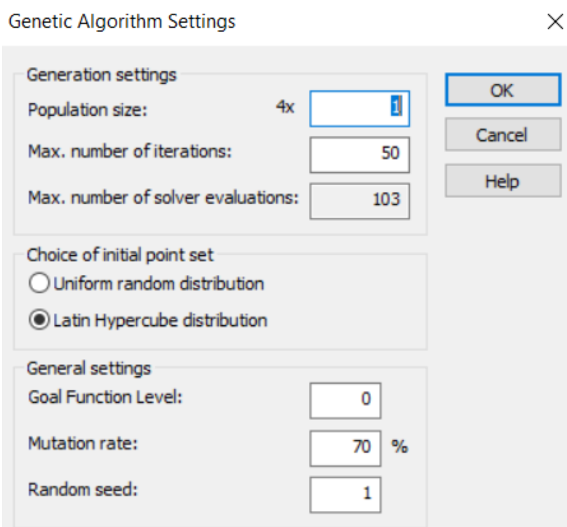

Şekil 6. Genetik algoritma parametre ayarları

Şekil 6'da genetik algoritmayla ilgili birçok parametre yer almaktadır. Bu parametrelerin özellikleri şöyle sıralanabilir:

"Population size" (nüfus boyutu): Genetik algoritmanın her bir iterasyonu veya jenerasyonu için kullanılan birey sayısını belirtir. Her bir birey, potansiyel bir çözümü temsil eder.

"Max. number of iterations" (maksimum iterasyon sayısı): Genetik algoritmadaki iterasyon yapısının ne kadar süreyle devam edeceğini belirler.

"Max. number of solver evoluations" (çözücü değerlendirmelerinin maksimum sayısı): Genetik algoritmanın belirli bir iterasyon sayısı içinde problemin çözümüne yönelik olarak gerçekleştirdiği değerlendirme veya hesaplamaların maksimum sayısını belirtir.

"Initial point set" (başlangıç noktası seti): Rastgele sayı dağılım türleri seçilir. "Uniform random distribution" (düzgün rastgele dağılım) belirli bir aralıktaki her değerin eşit olasılıkla seçilmesini sağlar. "Latin hypercube distribution" (Latin hiperküp dağılımı) ise her bir boyutta belirli bir aralıktaki değerin sadece bir kere seçilmesini sağlar. Bu dağılım her boyutta düzgün dağılmış örnekler elde etmek için kullanılır.

"Goal function level" (hedef fonksiyon seviyesi): Bu parametre; algoritmanın, maksimum iterasyon sayısına ulaşmadan hedefe ulaşması sonucunda durdurulmasını sağlayan hedefi belirtir. Eğer algoritma bu parametredeki değeri elde ederse algoritma maksimum iterasyona ulaşmadan kendini durduracaktır.

"Mutation rate" (mutasyon yüzdesi): Bu parametre, iki bireyin değeri birbirine yakın ise mutasyonun meydana gelme olasılığını belirler.

"Random seed" (rastgele tohum): Bu parametre programın rastgele sayı üreteci tarafından kullanılan başlangıç değeridir. Rastgele sayı üretecilerinin başlangıç değerine sahip olmasından dolayı bu değerin boş bırakılmaması gerekir.

2.3.2 Parçacık Sürüsü Optimizasyonu

Algoritma ilk olarak 1995 yılında Kennedy ve Eberhart tarafından önerilmiştir. [11] Parçacık sürüsü optimizasyonu balık, kuş gibi sürü halinde yaşamını sürdüren canlıların sosyal davranış biçimlerini kullanan popülasyon tabanlı algoritmadır [12].

Programda parçacık sürü optimizasyonu ile ilgili parametre ayarları Şekil 7'deki gibidir:

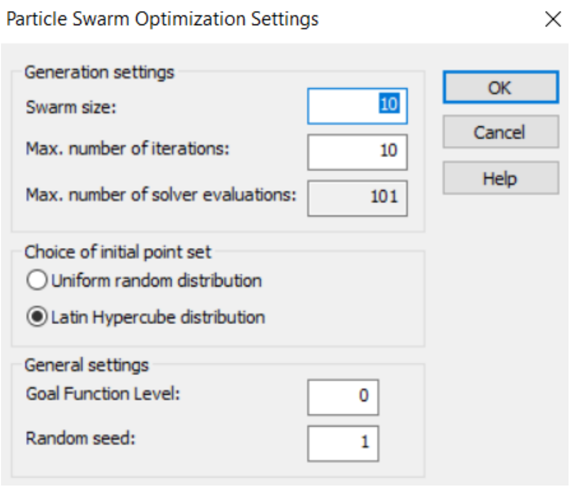

Şekil 7. Parçacık sürüsü optimizasyonu parametre ayarları

Şekil 7 incelendiğinde parçacık sürü algoritmasının ayarları genetik algoritmadaki ayarların çoğuna benzerdir. Tek farkı bu algoritmada sürü büyüklüğü olan "Swarm size" parametresidir. Bu parametre bir sürüdeki birey sayısını belirlemektedir. Maksimum iterasyon sayısı ile beraber bu algoritma sürüdeki her birey için 10 farklı çözüm oluşturur. Böylece 10 bireylik bir sürüde 10 iterasyonlu algoritmada 101 adet çözüm ortaya çıkar.

2.3.3 Parametre Taraması

Parametre taraması belirli bir simülasyon modelindeki parametrelerin farklı değerlerini otomatik olarak değiştirir ve her bir parametre kombinasyonu için simülasyonu yeniden çalıştırır. Tasarım sürecinde verimliliği artırmak ve tasarım seçeneklerini değerlendirmek için önemli bir araçtır.

Parametre taramasının gerçekleştirilmesi için öncelikle parametreler belirlenir. Ardından belirlenen parametrelerin hangi aralıkta taranacağı ve örnek sayısı tanımlanır. Tasarım parametrelerinin taranması ile ilgili 3 adet parametre hedeflenmiştir. Bu parametreler a katsayısı, Genişlik ve Uzunluk parametreleridir. a katsayısı parametresi 0,3 ila 0,7 arasında 9 örnek oluşturacak şekilde seçilmiştir. Genişlik ve Uzunluk parametreleri ise 120 mm ile 130 mm arasında 11 örnek oluşturacak şekilde girilmiştir.

2.4 Üretim Süreci

CST Studio Suite programında tasarlanan antenin üretilmesi için tasarımın baskısının alınması gerekir. Gerber dosyasını, ayarlanan koordinat yüzeyinde bulunan malzemeyi seçerek oluşturmak önemlidir. Yüzey materyali (örneğin; bakır) seçildikten sonra alınacak çıktı Şekil 8'deki gibi olacaktır. Şekil 9'da her iki yüzeyin çıktısı görülmektedir.

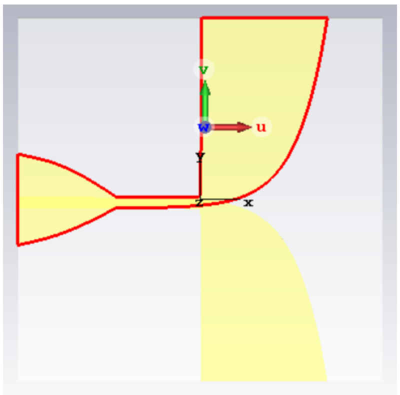

Şekil 8. Koordinat ayarlarından sonra seçilen yüzey

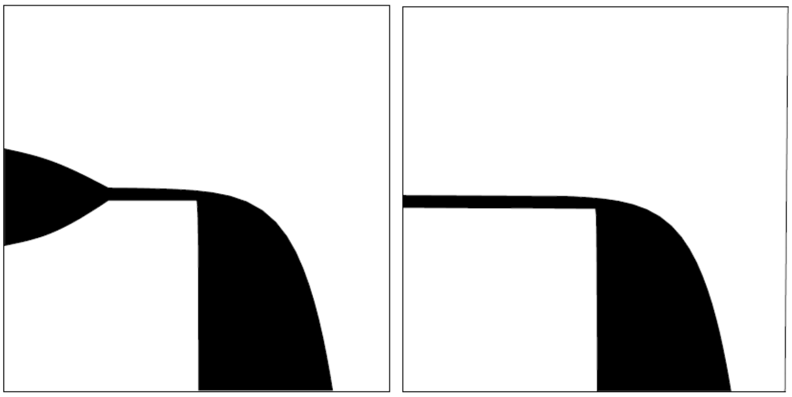

Şekil 9. PDF formatında çıkartılan tasarım dosyası

Üretim için çift tarafı 0,035 mm kalınlıkta bakır kaplı olan FR-4 plaketi kullanılmıştır. FR-4 plaketi CST Studio programında oluşturulan 1,5 mm kalınlığa sahiptir. Son olarak SMA port lehimlenerek anten nihai halini almıştır. Böylece anten, ölçüm alınması için hazır hale getirilmiştir.

2.5 Yöntem Süreçlerine Ait Çıktılar

Portun ayarlanması ile birlikte başlatılan simülasyon işlemi sonucunda oluşan S11 parametresi Şekil 10'da aktarılmıştır.

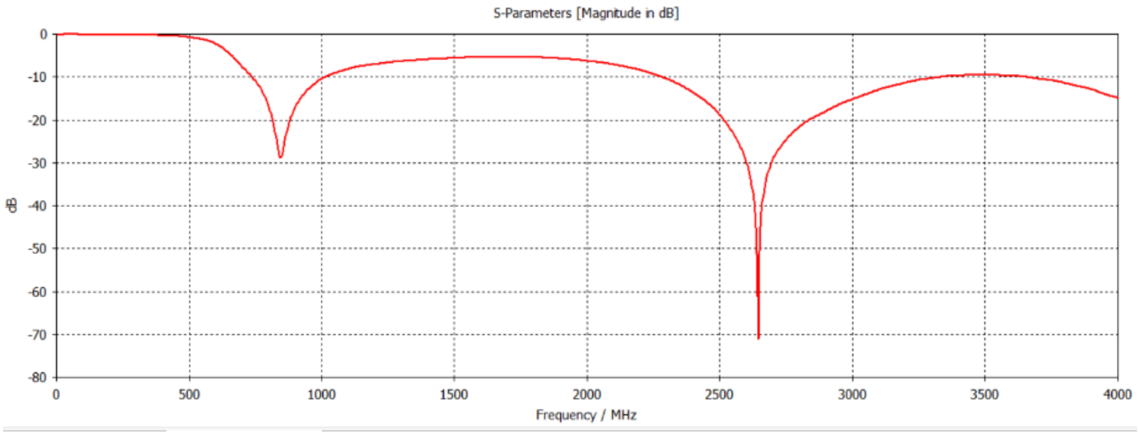

Şekil 10. S11 parametresi grafiği

Gerçekleştirilen ilk benzetimin ardından optimizasyon çalışmaları başlar ve ilk sonuçlar baz alınarak optimize edilecek değerler belirlenir. İlk optimizasyon olarak genetik algoritma optimizasyonu kullanılmıştır. Bu hususta elde edilen sonuç Şekil 11'deki gibidir:

```
Algorithm: Genetic Algorithm
103 of maximal 103 solver runs done

Number of evaluations: 103
          (solver: 102, reloaded: 1)
First goal function value   = 7.39719696238
Best goal function value    = 0.460749554557
Last goal function value    = 0.460749554557  (reloaded)

Last solver evaluation time = 00:03:25 h


Best parameters so far:

 a = 0.301785
 b = 0.09936
 Genislik = 110.653
 Uzunluk = 135.593
 W = 3.69333

(Corresponding run ID: 1382)
```

Şekil 11. Genetik algoritma sonuçları

Gerçekleştirilen benzetimde nüfus boyutu 1, maksimum iterasyon sayısı 50 olarak ayarlanmıştır. Geri kalan parametreler CST programının temel ayarlanmaları olarak bırakılmıştır. Sonuç olarak elde edilen optimizasyon grafiklerine Şekil 12'de yer verilmiştir.

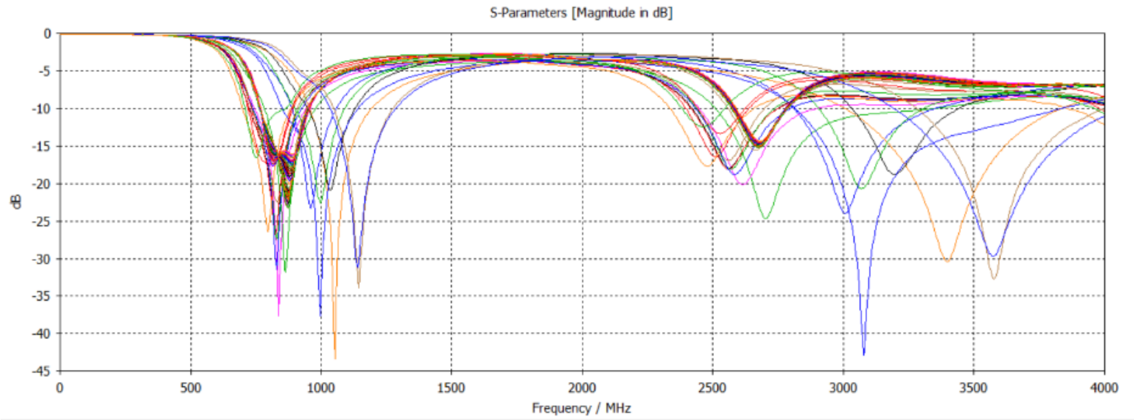

Şekil 12. Genetik algoritma sonuçlarına ait S11 grafikleri

Şekil 12'de yer alan grafikte genetik algoritma ile üretilen 100 adet çözüm görülmektedir. Elde edilen sonuçlar ve grafik incelendiğinde algoritmaya göre en iyi sonuç Şekil 13'teki gibidir:

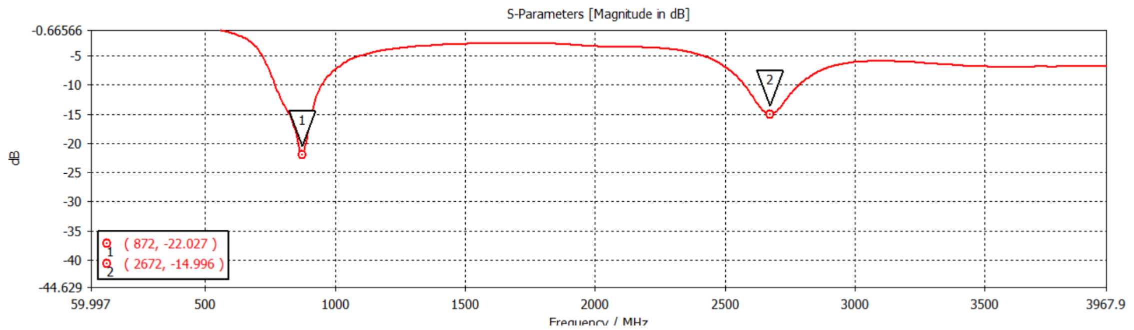

Şekil 13. Genetik algoritmaya göre en iyi sonuca ait grafik

Şekil 13'te en iyi sonucun elde edilmesi için anten tasarımında Genişlik ve Uzunluk parametrelerinin sırasıyla 110,65 mm ve 135,6 mm olması gerektiği anlaşılır. Ayrıca mikroşerit yolun kalınlığının 3,69 mm'ye indirilmesi, a ve b katsayılarının 0,301785 ve 0,09936 değerlerine göre ayarlanması gerektiğini gösterir.

Genetik algoritma optimizasyonu sonrası parçacık sürüsü optimizasyonu gerçekleştirilmiştir. Parçacık sürüsü optimizasyonuna ait grafik Şekil 14'deki gibidir:

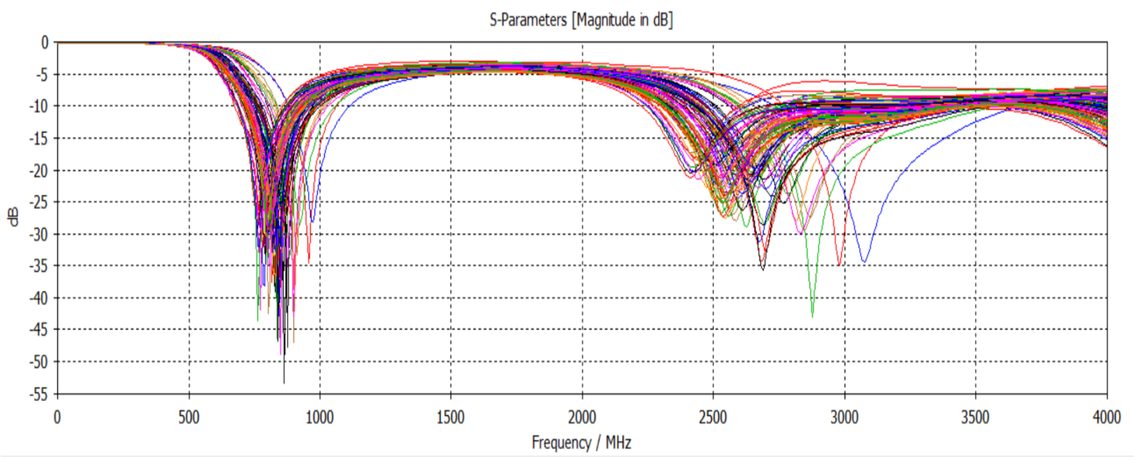

Şekil 14. Parçacık sürüsü optimizasyonu sonuçlarına ait S11 grafikleri

Şekil 14'de yer alan grafikte 100 adet sonuç yer almaktadır. Bu sonuçlar genetik algoritma ile kıyaslanırsa daha iyi performans gösteren anten parametrelerine sahip olduğu görülür. Grafikte 101 adet tarama bulunmaktadır. Optimizasyon tarafından en iyi sonuca ait parametre bilgileri Şekil 15'teki gibi açıklanmıştır.

```
Algorithm: Particle Swarm Optimization
101 of maximal 101 solver runs done

Number of evaluations: 101
              (solver: 100, reloaded: 1)
First goal function value   = 67.19694894
Best goal function value    = 28.7765992127
Last goal function value    = 28.7765992127  (reloaded)

Last solver evaluation time = 00:04:54 h


Best parameters so far:

 a = 0.497348
 b = 0.0131695
 Genislik = 146.71
 Uzunluk = 139.454
 W = 3.63868

(Corresponding run ID: 1560)
```

Şekil 15. Parçacık sürüsü optimizasyonu parametre sonuçları

Şekil 15'teki sonuca göre en iyi anten performans grafiği Şekil 16'da yer almaktadır.

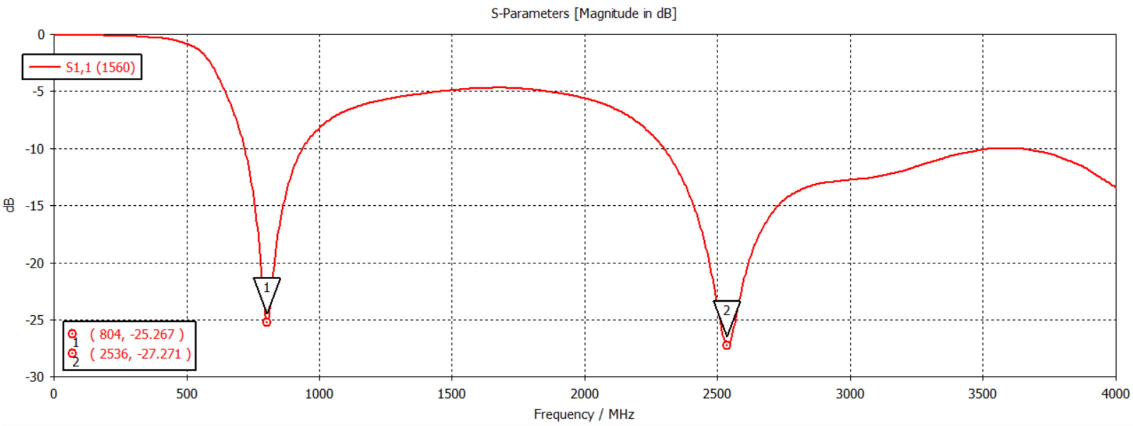

Şekil 16. Parçacık sürüsü optimizasyonu en iyi ölçüm sonucu

Bu durumda parçacık sürü optimizasyonuna göre anten performansı 804 MHz ve 2536 MHz noktalarında en iyi sonuca ulaşmaktadır. Bunun için anten tasarımında Genişlik ve Uzunluk parametreleri 146,71 mm ve 139,454 mm olmalıdır. Mikroşerit yolun kalınlığı 3,63868 mm değerinde olması gerekmektedir Aynı zamanda a ve b katsayılarının 0,497348 ve 0,0131695 değerlerinde olması gerekir.

Parçacık sürüsü optimizasyonu sonrasında parametre taraması işlemine geçilmiştir. Şekil 17'de yer alan ölçümler parametre taraması yöntemi ile gerçekleştirilmiştir. Tam olarak 1089 tarama bulunmaktadır. Her bir tarama girilen parametre ve adım sayısına göre artmaktadır.

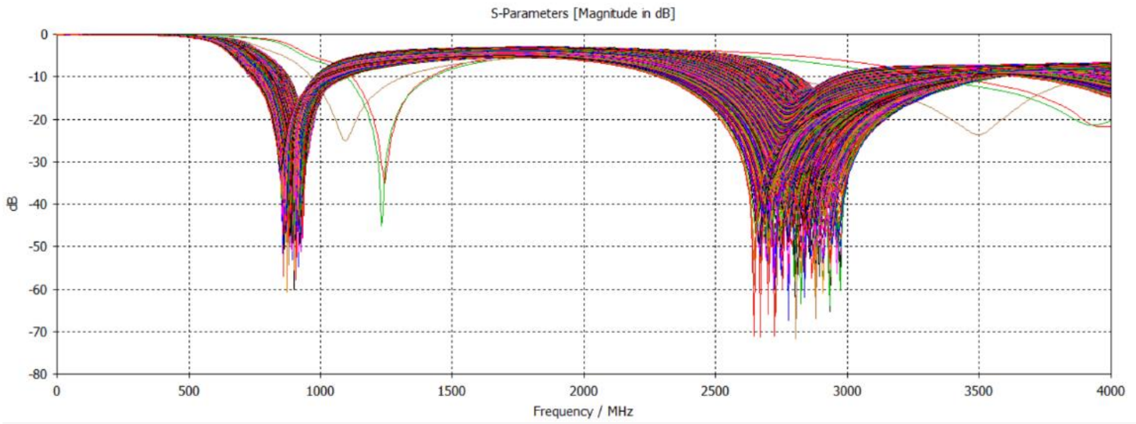

Şekil 17. Parametrik tarama ile gerçekleştirilen ölçümlerin sonuçlarına ait S11 grafikleri

Bu taramada girilen parametre sayısı 3'tür. Bunlar genişlik, uzunluk ve a katsayısı parametreleridir. Genişlik ve uzunluk parametleri 120 mm ile 130 mm arasında 11 adım olacak şekilde ayarlanmıştır. a katsayısı için ise 0,3 ile 0,7 arasında 9 adım olarak tanımlama yapılmıştır. Belirlenen bu değerler plaka boyutları ve frekans ilişkisi gereği seçilmiştir. Böylece toplam yapılacak olan tarama sayısı $11 \times 11 \times 9 = 1089$ olarak hesaplanmaktadır. Buna yönelik olarak en iyi sonuç veren parametre değerleri; genişlik: 130 mm, uzunluk 130 mm ve a 0,3 değerlerindedir. Bu değere ait grafik Şekil 18'de gösterilmiştir.

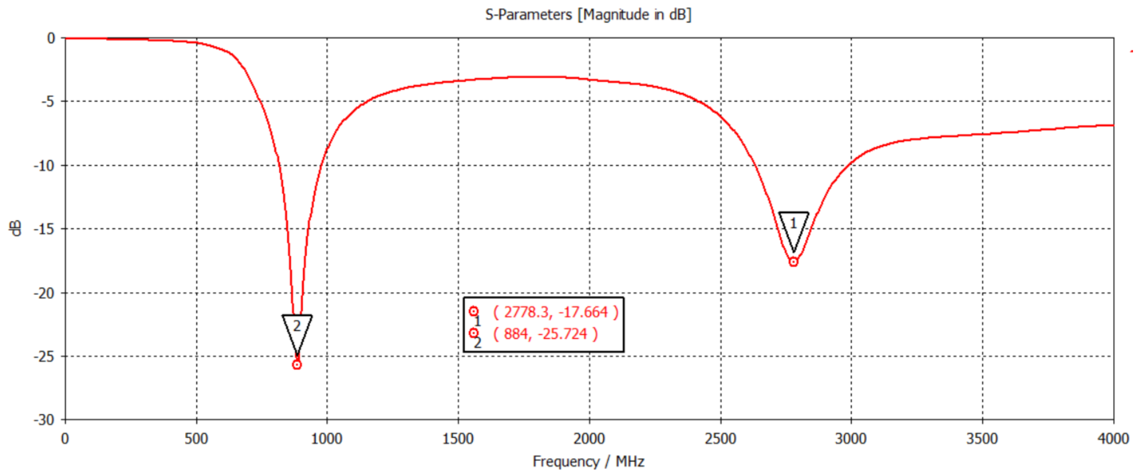

Şekil 18. Parametrik tarama sonrası en iyilenen anten boyutlarına göre S11 parametresi grafiği

3 Bulgular ve Tartışma

Benzetim grafiklerinden istenen sonuçlar alındıktan sonra laboratuvarda yapılacak olan gerçek ölçüm aşamalarına geçilmiştir. Tasarımı yapılıp baskısı alınan ve FR-4 plakaya aktarılan anten ile VNA cihazının bağlantısı Şekil 19'daki gibidir. Bağlantının gerçekleştirilmesinin ardından ilk olarak VNA'nın kalibrasyon ayarları gerçekleştirilmiştir. Bu yöntem, ölçüm cihazının doğru frekans tepkisini sağlamak ve ölçüm hatalarını minimize etmek amacıyla kullanılır [13]. Kalibrasyonlar gerçekleştirildikten sonra S parametreleri için ölçüm işlemi gerçekleştirilmiştir. Şekil 20'de S11 parametresine ait grafik yer almaktadır. S11 değeri, bir devre veya iletim hattının girişindeki yansımanın ölçüsüdür. Düşük S11 değerleri, daha az yansıma ve daha iyi bir eşleşme anlamına gelmektedir [14]. Optimizasyon yöntemleri sadece S11 değerini düşürmek için değil daha iyi yönlendirme sağlamak için de kullanılabilir. Yan lob seviyelerinin azalması üzerine yapılan bir çalışmada genetik algoritma kullanılmıştır [15]. Bu makale için a katsayısı, Genişlik ve Uzunluk değerlerinde parametrik tarama yönteminden elde edilen sonuçlara göre; mikroşerit yolun kalınlığı (W) ve b katsayısı için diğer tarama yöntemlerinden elde edilen bilgilere göre çıktı alınmıştır ve nihayetinde anten baskısı elde edilmiştir. Baskı hassasiyetinden ötürü 1 mm'den daha kısa olan uzunluklar 0'a yakın görülebilir. Uzunluklar kararlaştırılırken en iyi S11 değerlerine göre ve gerçeklenebilirliğe en uygun değerlere göre anten baskı uzunlukları ve katsayıları seçilmiştir.

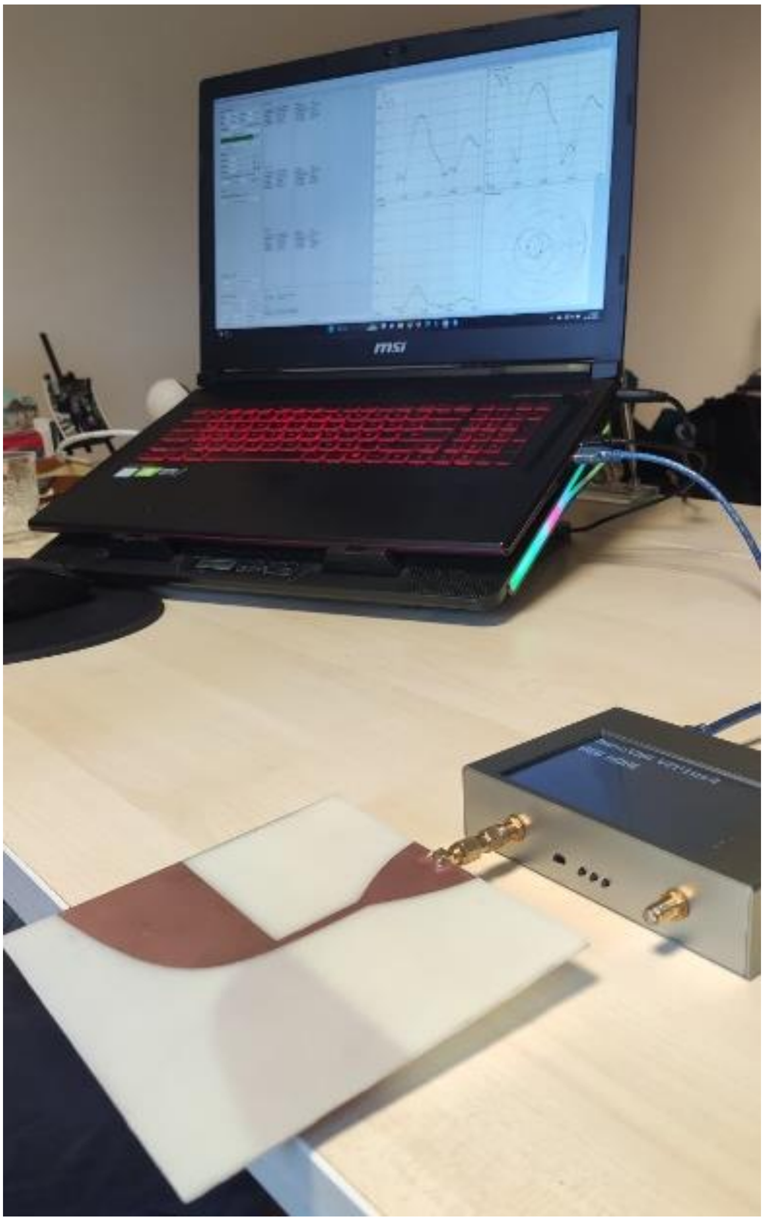

Şekil 19. Anten ile NanoVNA bağlantısı ve ölçüm alınması

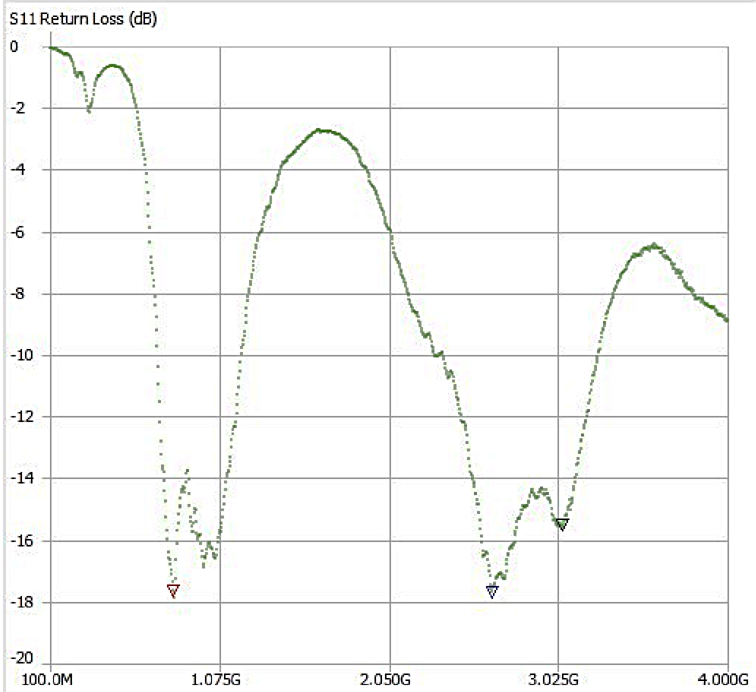

Şekil 20. S11 geri dönüş kaybı ölçümü

Şekil 20'de yer alan grafik incelendiğinde en düşük S11 değerleri 800 – 1000 MHz ile 2600 – 2700 MHz frekansları arasında gerçekleşmektedir. Şekil 21'de (Marker 1, Marker 2 ve Marker 3), Şekil 20 grafiğinde işaretlenen noktalara ait sayısal değerler yer almaktadır. Gerçekleştirilen antipodal Vivaldi anten tasarımı 807 MHz, 2643 MHz ve 3,05 GHz değerlerinde -15 dB'in altında bir değere ulaşmaktadır. En iyi çalışabilen merkez frekansın 2643 MHz frekans olduğu düşünülürse bu noktadaki S11 girişten geri yansıma değeri -17,719 dB'dir. Bant genişliği hesabında 3 yükseldiği noktalar arası belirlenmelidir. Bu demektir ki; -14,719 dB değerleri 2643 MHz frekansının solunda ve sağında aranacaktır. 2,53 GHz ve 2,77 GHz frekanslarında yaklaşık olarak -14,7 dB görülebilmektedir. Dolayısıyla; "Marker 2" ile gösterilen merkez frekansı 2643 MHz olan bölgenin 240 MHz bant genişliğine sahip olduğu anlaşılacaktır.

100 – 900 MHz aralığında çalışan, Şekil 1'deki Vivaldi anten tasarımına [8] çeşitli optimizasyon teknikleri uygulanarak oluşturulan yeni antenimizin sonuçlarının karşılaştırması yapıldığında S11 değeri daha da aşağılara inmiştir ve antenin çalışabileceği yeni frekans bantları oluşturulmuştur.

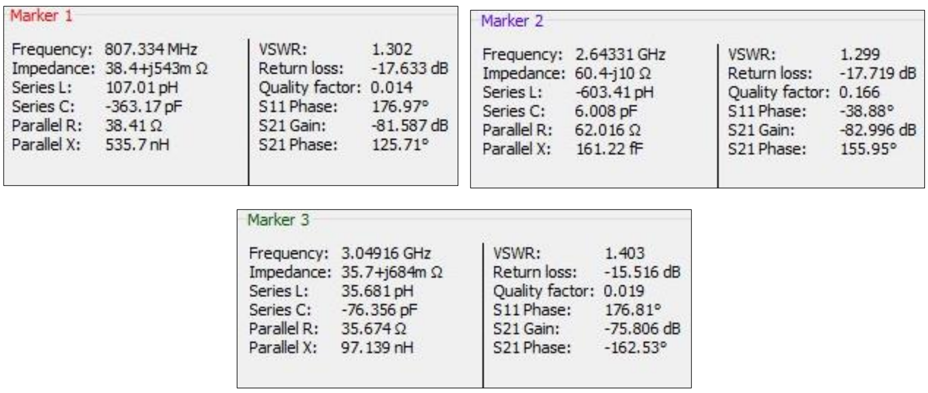

Şekil 21. S11 parametre grafiğindeki noktalara ait değerler

4 Sonuçlar

Bu çalışma, antipodal Vivaldi antenin; CST bilgisayar programı üzerinde tasarımını, optimizasyon algoritmaları ile en iyi sonucu elde etme işlemlerini, çift yüzeyi bakır kaplı FR-4 malzeme üzerine baskı devre aşamalarını ve NanoVNA cihazında ölçülmesi bölümlerini içermektedir. Temel hedef, antipodal Vivaldi tipindeki antenin istenen frekanslarda, 2G, 3G, 4G, 4.5G ve 5G gibi farklı mobil haberleşme teknolojileri ile tam uyumlu bir kapasiteyle çalışabilecek hale, optimizasyon algoritmalarıyla gelmesini sağlamaktır.

Yapılan ölçümler, testler ve iyileştirmeler sonucunda, geliştirilen antenin 807 MHz, 2643 MHz ve 3050 MHz frekanslarında -15 dB altındaki S11 değeri ile başarıyla çalıştığı tespit edilmiştir. Bu sonuçlar, antenin, frekans alt yapısı uygun olan ülkelerde farklı iletişim teknikleri ile uyum içinde kullanılabileceğini göstermektedir.

Antenin geniş spektrum uyumluluğu, mobil iletişim teknolojilerindeki çeşitliliğe yönelik taleplere cevap verebilme yeteneği vurgulanmıştır. Elde edilen sonuçlar, benzer uygulamalar ve iletişim sistemleri için temel teşkil edebilir ve gelecekteki kablosuz iletişim teknolojilerinin geliştirilmesine katkı sağlayabilir.

5 Beyanname

5.1 Rakip Çıkarlar

Bu çalışmada herhangi bir çıkar çatışması yoktur.

5.2 Yazarların Katkıları

Sorumlu Yazar Mehmet DUMAN: Araştırma ve makale için fikir ve hipotezin oluşturulması, sonuçlara ulaşmak için gereç ve yöntemlerin planlanması, ölçüm düzeneklerinin kurulması ve deneylerin yapılması, verilerin düzenlenmesi, bulguların açıklanması, yazının oluşturulması, imla ve dil bilgisi kontrolü aşamalarında katkı sunmuştur.
2. Yazar Volkan BERK: Sonuçlara ulaşmak için deneylerin yapılması, verilerin düzenlenmesi, denklemlerin kurulması, araştırma sırasında literatür taraması, kaynakçalandırma, yazının oluşturulması aşamalarında katkı sunmuştur.

Kaynakça

[1] Alsharif, M. H., Hossain, M. S., Jahid, A., Khan, M. A., Choi, B. J., & Mostafa, S. M. (2022). Milestones of Wireless Communication Networks and Technology Prospect of Next Generation (6G). Computers, Materials & Continua, 71(3).

[2] Thaiwirot, W., Kamoldej, D., Detchporn, P., Thongdit, P. & Tangwachirapan, S. (2022). Antipodal Vivaldi Antenna with Dielectric Lens for Biomedical Imaging Applications. IEEE Research, Invention, and Innovation Congress: Innovative Electricals and Electronics (RI2C), Bangkok, Thailand, pp. 93-96, doi: 10.1109/RI2C56397.2022.9910304.

[3] Wang, M., Crocco, L., Costanzo, S., Scapaticci, R. & Cavagnaro, M. (2022). A Compact Slot-Loaded Antipodal Vivaldi Antenna for a Microwave Imaging System to Monitor Liver Microwave Thermal Ablation. IEEE Open Journal of Antennas and Propagation, 3, pp. 700-708, doi: 10.1109/OJAP.2022.3183750.

[4] Kumar, S., & Dixit, A. (2022). Design of a high-gain dual-band antipodal Vivaldi antenna array for 5G communications. International Journal of Microwave and Wireless Technologies, 14(9), 1159-1167, doi:10.1017/S175907872100163X

[5] Wang, J., Liu, J., Hou, K., & Li, Y. (2023). A novel antipodal Vivaldi antenna for ultra-wideband far-field detection. AEU-International Journal of Electronics and Communications, 164, 154626.

[6] Muchhal, N., Vintimilla, R. Z., Fares, Y., & Elkhouly, M. (2023). Review on Recent Trends and Applications of Vivaldi Antenna in the Range of 1 GHz–40 GHz. The Fifteenth International Conference on Advances in Satellite and Space Communications.

[7] Stanley, M., Parker-Jervis, R., de Graaf, S., Lindström, T., Cunningham, J. E., & Ridler, N. M. (2022). Validating S-parameter measurements of RF integrated circuits at milli-Kelvin temperatures. Electronics Letters, 58(16), 614-616.

[8] Presse, A., Floc'h, J. M., Tarot, A. C. and Camus, C.. (2013). Broadband UHF flexible vivaldi antenna. Loughborough Antennas & Propagation Conference (LAPC), Loughborough, UK, pp. 277-280, doi: 10.1109/LAPC.2013.6711900.

[9] Di Trapani, F., Sberna, A. P., & Marano, G. C. (2022). A genetic algorithm-based framework for seismic retrofitting cost and expected annual loss optimization of non-conforming reinforced concrete frame structures. Computers & Structures, 271, 106855..

[10] Han, S., & Li, X. (2022). An improved adaptive genetic algorithm. In SHS Web of Conferences, 140. EDP Sciences.

[11] Xu, H. Q., Gu, S., Fan, Y. C., Li, X. S., Zhao, Y. F., Zhao, J., & Wang, J. J. (2023). A strategy learning framework for particle swarm optimization algorithm. Information Sciences, 619, 126-152.

[12] Gad, A. G. (2022). Particle swarm optimization algorithm and its applications: a systematic review. Archives of computational methods in engineering, 29(5), 2531-2561.

[13] Duan J. & Zhu L. (2022). Numerical Short-On-Load (SOL) Calibration Technique for Accurate Extraction of Electrically-Small Planar/Non-Planar Microstrip-Line Circuits. IEEE Transactions on Microwave Theory and Techniques, 70(4), pp. 2067-2076, doi: 10.1109/TMTT.2022.3143947.

[14] Cheng, J., Zhang, H., Ning, M., Raza, H., Zhang, D., Zheng, G., ... & Che, R. (2022). Emerging materials and designs for low-and multi-band electromagnetic wave absorbers: the search for dielectric and magnetic synergy? Advanced Functional Materials, 32(23), 2200123.

[15] Satılmış, G. (2022). Genetik Algoritma Kullanarak Dipol Dizi Antenlerde Yan Lob Bastırma. Muş Alparslan Üniversitesi Mühendislik Mimarlık Fakültesi Dergisi, 3(2), 50-56.

Research Paper
Journal of Smart Systems Research (JOINSSR) 5(1),33-39,2024
Received: 17-March-2023 Accepted: 23-May-2024
10.58769/joinssr.1453584

SAKARYA UNIVERSITY OF APPLIED SCIENCES

A Low-Cost Soft Gripper for Automated Pick-and-Place Systems

Mert Süleyman DEMİRSOY[1], Metin Eren ATALAY[1], Ardi Billurdagi[1], Mustafa Çağrı KUTLU[1*]

[1] Mechatronic Engineering, Faculty of Technology, Sakarya University of Applied Sciences

ABSTRACT

The study introduces a pioneering low-cost soft gripper designed for the automation industry, specifically targeting sensitive handling requirements in the food and health sectors. Utilizing rubber or elastic composites, the gripper combines improved sensitivity and adaptability to handle delicate materials safely and efficiently, aligning with stringent industry standards. Central to the design is a pneumatic control system that ensures precise manipulation, allowing the gripper to adapt to varying object contours without causing damage. This innovation not only addresses the mechanical aspects of soft robotics but also integrates seamlessly with Industry 4.0 technologies through smart sensors and AI algorithms, enhancing operational intelligence and versatility. By leveraging additive manufacturing techniques, the design also achieves significant cost reductions, facilitating broader adoption. This study's soft gripper represents a critical step forward in the development of robotic systems that can perform complex tasks with high sensitivity and economic efficiency, promising transformative impacts on the automation capabilities of sensitive industrial sectors.

Keywords: Soft Robotics, Gripper Design, Pick-and-Place

1 Introduction

The inception of the Industrial Revolution marked the beginning of significant advancements in manufacturing, culminating in the creation of the first programmable robot in 1954. Today, the field of robotics faces new challenges, particularly in handling delicate materials safely and efficiently. Soft robotics, inspired by the adaptive nature of biological organisms, presents solutions to these challenges. Our work introduces a novel soft gripper that addresses the need for gentle handling in the automation industry without compromising on precision or cost [12].

Recent advancements in soft robotics have predominantly focused on the development of soft actuators and grippers, reflecting a growing recognition of their potential to revolutionize industrial automation, particularly in pick-and-place systems. Soft grippers, fabricated from materials such as silicone, exhibit unparalleled flexibility and adaptability, enabling the gentle handling of a wide range of objects, from fragile components to irregularly shaped food products [5,10]. These characteristics have catalyzed significant research into the optimization of soft gripper design for enhanced performance and cost-efficiency.

* Corresponding Author's email: mkutlu@subu.edu.tr

The literature is replete with studies exploring various facets of soft gripper innovation. For instance, experiments with inflatable membranes [6] and the development of versatile gripping systems [8] have expanded the functional capabilities of soft grippers. Further, research into the simulation of elastomer actuators [9] and the utilization of shape memory materials [13] has enriched our understanding of the materials science underpinning soft robotics. The integration of pneumatic double-joint actuators has also been explored, enhancing the dexterity and efficiency of soft gripping mechanisms [16].

Current soft grippers, while versatile, often fall short in balancing cost, efficiency, and delicate handling capabilities. Our research addresses these gaps by developing a cost-effective, highly adaptable gripper that meets the rigorous demands of sensitive industrial environments. This means the field faces challenges in the form of high manufacturing costs and complexity in design and control systems, which hinder the broader adoption of soft grippers in industrial applications. Addressing these challenges, the current study aims to design and develop a new soft robot gripper that leverages low-cost additive manufacturing techniques without compromising on efficiency or functionality. This research endeavors to bridge the gap between the theoretical potential and practical implementation of soft grippers, focusing on system overview, mechanical design, pneumatic control, and automation design. It seeks to underscore the cost-effectiveness and usability of the new design, thereby contributing a novel solution to the ongoing discourse in soft robotics.

2 Materials and Methods

The genesis of the proposed soft gripper system was predicated on a foundational design philosophy that emphasizes cost-efficiency, ease of manufacturing, and operational versatility. Utilizing computer-aided design (CAD) software, the initial geometric and structural parameters of the gripper were conceptualized as shown in Figures 1 and 2. This phase was informed by an extensive review of biomimetic principles, aiming to emulate the adaptive grip dynamics observed in natural organisms [6]. The design intricacies were further refined through iterative simulations, ensuring optimal force distribution and material elasticity for handling a variety of objects. To evaluate the gripper's performance, we employed a series of empirical tests and simulations. Detailed parameters, such as air pressure ranges and grip force settings, were documented to ensure reproducibility. Our experiments simulated real-world pick-and-place tasks to validate the gripper's functionality across various object types.

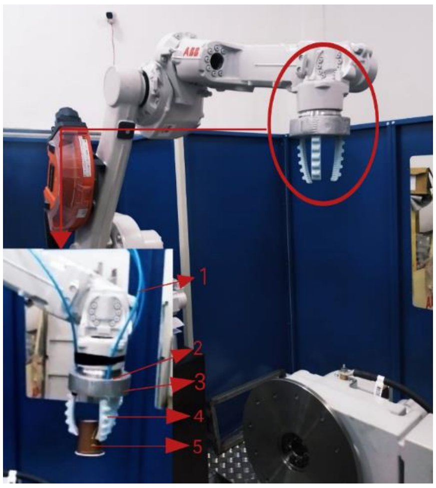

Figure 1. System Components

2.1 Fabrication and Material Selection

The fabrication process leveraged state-of-the-art additive manufacturing techniques, specifically fused deposition modeling (FDM), to prototype the gripper components with mold (PLA). A critical selection criterion for the gripper material was its elasticity and durability, leading to the choice of a custom-formulated silicone composite (RTV-2 Shore 20 Silicone, 10x20x150 mm). This material exhibited excellent deformation recovery and high tensile strength, essential for the gripper's repeated use in industrial settings [5].

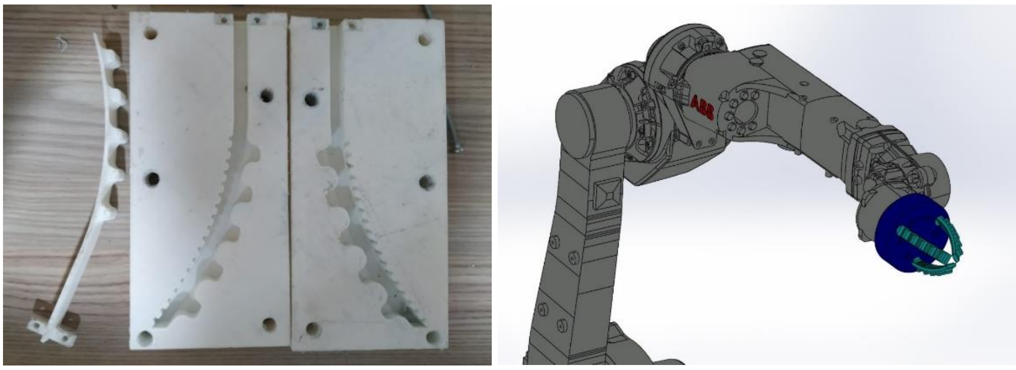

Figure 2. (a) Mold design holder shape and core (b) CAD Model of the Assembled Soft Gripper

2.2 Pneumatic Control System

Central to the gripper's operation is a pneumatic control system designed to modulate the grip force and actuation speed. The system's architecture was developed using Pneumatic Studio software, enabling precise control over the air flow and pressure within the gripper's chambers. This setup allowed for the gripper's adaptive functionality, accommodating objects of varying shapes and fragility as shown in Figure 3 [10].

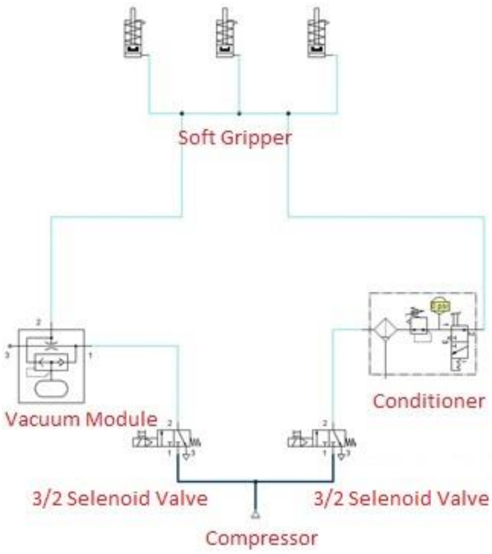

Figure 3. Pneumatic Control System Schematic

2.3 Testing and Evaluation

The gripper's performance was rigorously evaluated through a series of empirical tests, assessing its grip strength, object handling versatility, and operational durability. A bespoke testing rig was constructed, simulating real-world pick-and-place scenarios across a spectrum of object types, from delicate glassware to irregularly shaped produce. The evaluation process was augmented by finite element analysis (FEA) in ANSYS Workbench, providing insights into stress distribution and potential material fatigue under repeated use conditions in Figure 4.

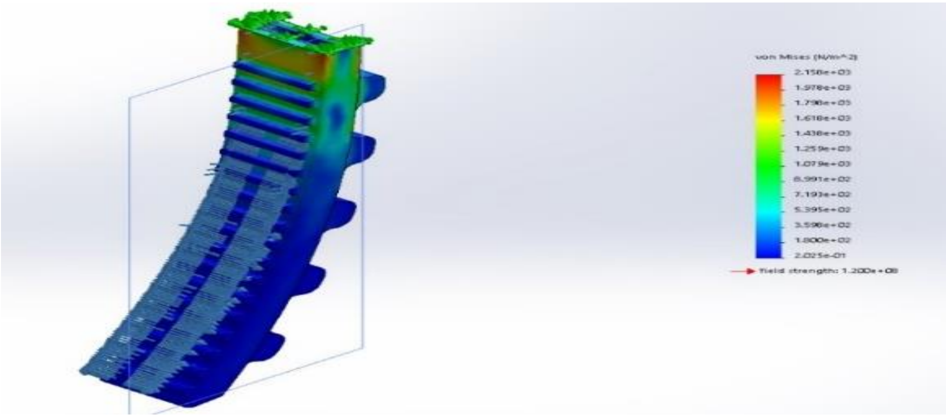

Figure 4. Pneumatic simulations with FEA

Another important topic while designing Soft gripper is ease of use. So that it is intent to carry out the transport process without deforming it. To ensure that the gripper switches on and off automatically, a mechanical trigger is required first. The solenoid valve performs this process. To receive the valve signal, we must first physically connect the inputs and outputs to the controller. In order for these connections to work synchronously with the robot, we have to define the inputs and outputs, as shown in Figure 5, which we have connected by receiving from the controller part in the Robostudio to the signal part via the I / O system. As show in Figure 5, the I / O signal part is defined which enables the controllers to operate synchronously.

Figure 5: Robotstudio smart components

3 Results and Discussions

The implementation of the novel soft gripper design was subjected to a rigorous empirical evaluation to ascertain its mechanical integrity, operational efficiency, and adaptability in handling diverse materials. The pneumatic actuation mechanism, central to the gripper's functionality, facilitated a responsive and adaptable gripping action, characterized by its ability to modulate force based on the object's geometry and material composition [14]. The bending angles and deformation under varying loads were systematically recorded, revealing the gripper's capacity for significant mechanical flexibility and durability under operational stresses [4].

Parallel to mechanical testing, simulation exercises employing advanced computational models offered predictive insights into the gripper's performance across a spectrum of operational scenarios. These simulations, validated through subsequent real-world applications, underscored the gripper's proficiency in executing precise and delicate pick-and-place tasks, thus substantiating its utility in industrial settings where such capabilities are paramount as shown in Figure 6 [2].

The real-world applicability of the soft gripper was further evidenced through a series of controlled experiments focusing on the manipulation of fragile items, such as glassware and perishable goods. These tests demonstrated not only the gripper's adept handling but also its potential to mitigate the risk of product damage, thereby enhancing operational safety and efficiency [11].

A pivotal aspect of the soft gripper's development was its economic feasibility. A comprehensive cost analysis revealed the production costs of the soft gripper to be significantly lower than those associated with conventional robotic grippers, highlighting its potential for widespread adoption across various sectors of the manufacturing industry [8]. This cost efficiency, coupled with the gripper's demonstrated performance, underscores its value proposition as a transformative tool in the automation landscape.

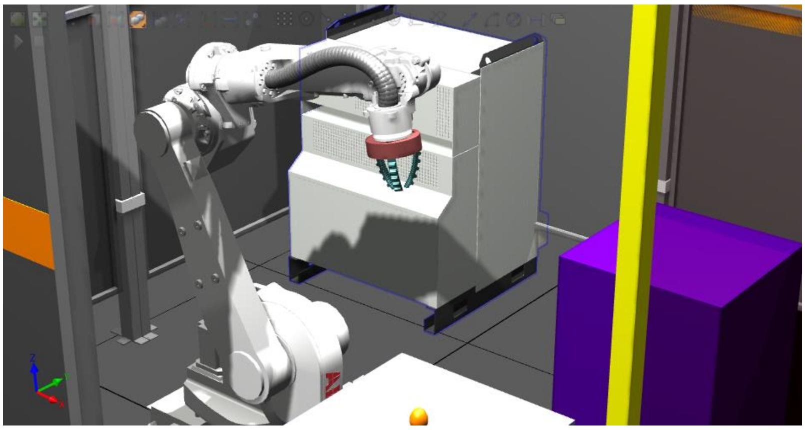

Figure 6. Automation simulation from robotstudio

The results presented herein, supported by rigorous empirical testing and comprehensive cost analysis, affirm the soft gripper's potential to redefine efficiency and safety in automated pick-and-place operations. Notably, the integration of low-cost materials and innovative design principles contribute to a paradigm shift in the approach to robotic manipulation, particularly in industries where the handling of delicate or irregularly shaped objects is commonplace. Future investigations will aim to extend the gripper's capabilities, incorporating advanced sensor technologies and AI-driven control algorithms to further enhance its adaptability and operational intelligence [7].

4 Conclusions

This study has successfully demonstrated the design, implementation, and validation of a low-cost soft gripper, tailored for industrial applications, especially in automating pick-and-place tasks. The utilization of RTV-2 molded silicone, in conjunction with a pneumatic actuation system, has yielded a gripper capable of delicate and precise object manipulation. This approach not only minimizes potential damage to the objects handled but also introduces a degree of dexterity reminiscent of human hand movements, thereby expanding the operational capabilities of industrial robot arms [1].

Our findings highlight the soft gripper's potential to reduce operational costs and enhance safety in automated systems. The gripper's low production costs and high functionality make it a viable alternative for industries requiring delicate object handling. Furthermore, the application of the finite element method (FEM) for system analysis has substantiated the gripper's operational efficiency under designated pressure ranges, thereby affirming its suitability for varied industrial tasks [3,17].

The potential for innovation within the realm of soft robotics remains vast. Future research will endeavor to integrate advanced sensory feedback mechanisms into the soft gripper design, enabling more sophisticated object recognition and manipulation capabilities. The exploration of smart materials with enhanced actuation properties and resilience could further augment the gripper's adaptability and longevity. Moreover, the integration of machine learning algorithms promises to refine the gripper's decision-making processes, facilitating autonomous adjustments to grip strength and technique based on real-time assessment of object characteristics. This advancement will not only increase the operational efficiency of automated systems but also expand their applicability to more complex and nuanced tasks.

Future research will focus on integrating sensory feedback to enhance object recognition and manipulation. We also plan to explore smart materials to further improve the gripper's performance and durability. Tailoring gripper designs to cater to the unique demands of sectors such as healthcare, agriculture, and consumer goods could unlock new possibilities for automation technologies, driving further innovations in Industry 4.0 applications.

5 Declarations

5.1 Competing Interests

There is no conflict of interest in this study.

5.2 Authors’ Contributions

1. MEA: Organizing and reporting the data, taking responsibility for the explanation and presentation of the results,

2. AB: taking responsibility for the experiments, taking responsibility for the creation of the entire manuscript.

3. MSD: Taking responsibility for the literature review during the research, taking responsibility for the explanation and presentation of the results, taking responsibility for the experiments.

4. MK: Developing ideas or hypotheses for the research and article, planning the materials and methods to reach the results, supervising.

References

1. V. Cacucciolo, J. Shintake, D. Floreano, and H. Shea, "Soft robotic grippers," Advanced Materials, vol. 30, no. 29, Art. no. 1707035, 2018, https://doi.org/10.1002/adma.201707035.
2. Wang, Boran, et al. "Design, modelling and simulation of soft grippers using new bimorph pneumatic bending actuators." Cogent Engineering 4.1 (2017): 1285482.
3. J. M. Jin, The Finite Element Method in Electromagnetics, John Wiley & Sons, 2015.
4. Ye, Yuze, et al. "Design of a novel soft pneumatic gripper with variable gripping size and mode." Journal of Intelligent & Robotic Systems 106.1 (2022): 5.
5. S. Kim, C. Laschi, and B. Trimmer, "Soft robotics: a bioinspired evolution in robotics," Trends in Biotechnology, vol. 31, no. 5, pp. 287–294, 2013.
6. C. Laschi, B. Mazzolai, and M. Cianchetti, "Soft robotics: Technologies and systems pushing the boundaries of robot abilities," Science Robotics, vol. 1, no. 1, eaah3690, 2012.
7. Qu, Juntian, et al. "Recent progress in advanced tactile sensing technologies for soft grippers." Advanced Functional Materials 33.41 (2023): 2306249.
8. C. Majidi, "Soft robotics: a perspective—current trends and prospects for the future," Soft Robotics, vol. 1, no. 1, pp. 5–11, 2014.
9. B. Mosadegh, P. Polygerinos, C. Keplinger, S. Wennstedt, R. F. Shepherd, U. Gupta, J. Shim, K. Bertoldi, C. J. Walsh, and G. M. Whitesides, "Pneumatic networks for soft robotics that actuate rapidly," Advanced Functional Materials, vol. 24, no. 15, pp. 2163–2170, 2014.
10. P. Polygerinos, Z. Wang, K. C. Galloway, R. J. Wood, and C. J. Walsh, "Soft robotic glove for combined assistance and at-home rehabilitation," Robotics and Autonomous Systems, vol. 73, pp. 135–143, 2015.
11. Sinatra, Nina R., et al. "Ultragentle manipulation of delicate structures using a soft robotic gripper." Science Robotics 4.33 (2019): eaax5425..
12. D. Rus and M. T. Tolley, "Design, fabrication, and control of soft robots," Nature, vol. 521, no. 7553, pp. 467–475, 2015.
13. R. F. Shepherd, F. Ilievski, W. Choi, S. A. Morin, A. A. Stokes, A. D. Mazzeo, X. Chen, M. Wang, and G. M. Whitesides, "Multigait soft robot," Proceedings of the National Academy of Sciences, vol. 108, no. 51, pp. 20400–20403, 2011.
14. Manti, Mariangela, et al. "A bioinspired soft robotic gripper for adaptable and effective grasping." Soft Robotics 2.3 (2015): 107-116.
15. Wan, Fang, et al. "A reconfigurable design for omni-adaptive grasp learning." IEEE Robotics and Automation Letters 5.3 (2020): 4210-4217.
16. M. T. Tolley, R. F. Shepherd, B. Mosadegh, K. C. Galloway, M. Wehner, M. Karpelson, R. J. Wood, and G. M. Whitesides, "A resilient, untethered soft robot," Soft Robotics, vol. 1, no. 3, pp. 213–223, 2014.
17. O. C. Zienkiewicz, R. L. Taylor, P. Nithiarasu, and J. Z. Zhu, The Finite Element Method:Its Basis and Fundementals, vol. 3, McGraw-hill, London, 1977.

Research Paper
Journal of Smart Systems Research (JOINSSR) 5(1),40-54,2024
Received: 8-May-2024 Accepted: 4-June-2024
DOI: 10.58769/joinssr.1480695

SAKARYA UNIVERSITY OF APPLIED SCIENCES

Assessing Student Success: The Impact of Machine Learning and XAI-BBO Approach

Cem ÖZKURT[1,2*]

[1] Department of Computer Engineering, Faculty of Technology, Sakarya University of Applied Sciences
[2] Artificial Intelligence and Data Science Application and Research Center, Sakarya University of Applied Sciences

ABSTRACT

In today's dynamic educational landscape, understanding the multifaceted factors contributing to student success is paramount. This study delves into the intricate interplay of various determinants affecting student achievement. Through comprehensive preprocessing techniques, including nuanced transformations of categorical variables such as gender, age range, and parental education level, this research endeavors to unravel the complex fabric of educational outcomes. Leveraging the Biogeography-Based Optimization (BBO) algorithm, pivotal features crucial to student success are identified and integrated into sophisticated machine learning models. Evaluation metrics encompassing Accuracy, Precision, Recall, and F1 score illuminate the efficacy of these models, with the Gradient Boosting algorithm emerging as a standout performer, attaining a notable Accuracy value of 0.7388, Precision of 0.75, Recall of 0.72, and F1 score of 0.74. Further insights into model interpretability are gleaned through the application of SHAP and LIME methodologies, shedding light on the intricate mechanisms driving predictive outcomes. Specifically, the SHAP analysis highlights the influential factors driving model predictions, while LIME provides valuable insights into individual feature contributions. This study underscores the imperative of meticulous examination in delineating the determinants of student achievement, advocating for continued inquiry to inform evidence-based educational policies. The discernments furnished herein hold promise for fostering data-driven decision-making frameworks in education and facilitating targeted interventions aimed at fostering student success.

Keywords: Biogeography-Based Optimization (BBO) algorithm, Machine Learning models, Gradient Boosting algorithm, SHAP method, LIME method

1 Introduction

This study was conducted to analyze and explain the complex socio-economic factors that determine student success. In educational systems, there are many variables that affect student achievement, with socio-economic factors being of great importance among these variables [1]. Socio-economic factors such as family income level, parental education level, and living conditions can influence a student's academic performance.

In this research, various preprocessing steps were applied to the dataset to enable more effective use of categorical variables. Specifically, categorical variables in string type were converted to integer types to enhance the processing efficiency of the models. These significant adjustments included variables such as students' gender, age range, and parents' education level. The use of the Biogeography-Based Optimization (BBO) algorithm in the analysis of the dataset proved effective in identifying complex

[1] Corresponding Author's email: cemozkurt@subu.edu.tr

relationships and allowed for the selection of attributes according to the complexity among features. In this study, using the BBO algorithm, the 20 most influential attributes affecting student success were identified from among the 32 attributes in the dataset.

These important attributes were evaluated by including them in machine learning models and using metrics such as Accuracy, Precision, Recall, and F1-score. The Gradient Boosting algorithm, which had the best Accuracy value, was explained using interpretable artificial intelligence models such as SHAP and LIME. The results obtained from this study emphasized the need for a detailed examination of the factors influencing student success and indicated the necessity for further research to enable more effective formulation and implementation of education policies. The findings of this study could contribute to the development of data-driven decision-making processes in the field of education and to more effectively planning interventions to improve student success.

2 Literature Review

One study examined the socioeconomic factors influencing the academic achievements of middle school students in Pakistan [2]. This study revealed that the education level of parents and socioeconomic status significantly impact students' performance in mathematics and English.

Another study conducted in Australia analyzed longitudinal data to explore factors affecting student achievement [3]. It demonstrated that prior achievements and early childhood cognitive abilities are crucial determinants of student success, with limited influence from socioeconomic status.

There is a study recommending the use of a type of Biogeography-based Optimization (BBO) in feature selection problems [4]. BBO relies on mathematical equations used to model the geographical distribution of biological organisms. Researchers propose that combining BBO with Support Vector Machine Recursive Feature Elimination (SVM-RFE) could create a more effective hybrid model for feature selection problems, leading to higher performance and better results in these problems.

Another study examines the impact of using artificial neural networks (ANNs) in education [5]. Researchers evaluate how effective multi-layer perceptron artificial neural networks (MLP-ANNs) are in predicting student performance. The study shows that multi-layer perceptron artificial neural networks developed considering students' past academic achievements and other factors have a high success rate in predicting student performance.

There is also a study that uses machine learning algorithms to predict the academic performance of students in a high school in Turkey [6]. Researchers evaluate various machine learning algorithms, including K-Nearest Neighbor, Decision Trees, Random Forest, Support Vector Machines, Multi-layer Perceptron, Logistic Regression, and Naive Bayes, using a dataset of 655 students. The results indicate that the Random Forest algorithm achieves the highest success rate. This study provides an effective machine learning model for predicting the academic performance of high school students in Turkey.

A model was developed using machine learning algorithms to predict the academic achievements of students in a high school in Turkey [7]. Evaluating seven different machine learning algorithms, including K-Nearest Neighbors, Decision Trees, Random Forests, Support Vector Machines, Multi-Layer Perceptron, Logistic Regression, and Naive Bayes, using a dataset of 655 students, the study found Random Forest algorithm to have the highest success rate.

A framework was proposed to provide career counseling to students using machine learning and artificial intelligence techniques [8]. The study examined how white-box and black-box models could analyze educational data to offer career advice to students, with Naive Bayes identified as the most effective model.

A systematic review was conducted on interpretable student performance prediction models between 2015 and 2020 [9]. The review examined various studies in the literature and discussed how interpretable student performance prediction models could be developed, summarizing different research methods and findings and providing recommendations for future research.

A study aimed to improve decision support systems using local interpretable machine learning modeling to predict student attrition [10]. By developing a model using a large dataset to predict students' academic performance and enrollment status, the study enhanced the accuracy of decision support systems and facilitated the identification of more effective interventions.

An investigation was described, employing artificial intelligence methods to assess academic achievement in general high schools in a European Union country [11]. The study developed a model using artificial intelligence algorithms to measure the academic achievements of general high school students, considering various factors to predict students' academic performance and provide a criterion for determining their success.

3 Materials And Methodology

In this section, a dataset encompassing socio-economic and personal factors influencing students' academic achievements was employed, comprising parameters such as gender, age, parental education levels, family structure, residence type, commute time to school, study duration, social activities, alcohol consumption, health status, and prior semester grades. Biogeography-Based Optimization (BBO) algorithm was utilized for feature selection, inspired by natural migration and distribution processes of species. Within the realm of machine learning, Artificial Neural Networks (ANN), XGBoost, LightGBM, Random Forest (RF), Support Vector Machine (SVM), K-Nearest Neighbors (KNN), and Gradient Boosting algorithms were deployed, serving as data-driven modeling techniques to predict student success.

3.1 Dataset

In this study, a dataset containing socio-economic and personal factors affecting students' academic achievements has been utilized. The dataset includes parameters such as the student's gender, age, parents' education levels, family structure, type of residence, travel time to school, study duration, social activities, alcohol consumption, health status, and previous semester grades. An example of the dataset is provided in Figure 1.

	school	sex	age	address	famsize	Pstatus	Medu	Fedu	Mjob	Fjob	...	famrel	freetime	goout	Dalc	Walc	health	absences
0	GP	F	18	U	GT3	A	4	4	at_home	teacher	...	4	3	4	1	1	3	6
1	GP	F	17	U	GT3	T	1	1	at_home	other	...	5	3	3	1	1	3	4
2	GP	F	15	U	LE3	T	1	1	at_home	other	...	4	3	2	2	3	3	10
3	GP	F	15	U	GT3	T	4	2	health	services	...	3	2	2	1	1	5	2
4	GP	F	16	U	GT3	T	3	3	other	other	...	4	3	2	1	2	5	4
...	...	...	...	...	...	...	...	...	...	...	...	...	...	...	...	...	...	...

Figure 1: Example of raw data set used in the study.

3.2 Biogeography-Based Optimization (BBO)

The Biogeography-Based Optimization (BBO) algorithm is defined as an optimization algorithm developed by drawing inspiration from nature, modeling the migration and distribution processes of species to solve optimization problems. In the context of feature selection, BBO allows for the identification of the most important features by evaluating their contribution to the desired outcome. By simulating the natural migration process of species, BBO effectively explores the feature space and selects the features that have the greatest impact on the desired outcome [12].

3.3 Machine Learning

Machine learning is considered as a branch of artificial intelligence where computer systems are enabled to learn from data-driven experiences to solve complex problems. This method relies on algorithms having the capability to learn automatically from data in order to accomplish a specific task. Algorithms typically acquire knowledge by identifying patterns using large amounts of data and can make predictions or decisions based on these patterns. Machine learning intersects the fields of artificial intelligence and data science, and finds applications in various domains including image recognition, natural language processing, medical diagnosis, financial forecasting, and automation [13]. In this study, the Artificial Neural Networks (ANN), XGBoost, LightGBM, Random Forest (RF), Support Vector Machine (SVM), K-Nearest Neighbors (KNN), and Gradient Boosting algorithms were utilized.

3.3.1 Artificial Neural Networks (ANN)

Artificial Neural Networks (ANN) are artificial intelligence models designed by drawing inspiration from biological neural networks in computer systems. These networks are based on structures that mimic the functioning of neurons in the human brain and are typically multi-layered. They are used to perform complex tasks such as data analysis and pattern recognition. ANNs can perceive and learn patterns in datasets, allowing them to make predictions or classifications. During the training process, the network is presented with large amounts of data, and it learns by adjusting its internal weights and structures based on this data. As a result, ANNs are widely used in various fields such as image recognition, natural language processing, speech recognition, and autonomous driving [14]. The formula equation 1, which describes the working structure of Artificial Neural Networks, is provided.

$$z = \sum_{i=1}^{n} w_i x_i + b \tag{1}$$

In equation 1, z represents the output of the neuron, which signifies the weighted sum of inputs. w_i denotes the weight of input i, indicating the importance assigned to that input. x_i represents the value of input i. b signifies the bias value, a constant added to the output of the neuron. n indicates the total number of inputs. These equations are used to compute the weighted sum of inputs for a neuron in artificial neural networks, determining the neuron's output.

3.3.2 XGBOOST

XGBoost is a widely used algorithm in recent years in machine learning, often preferred for solving classification and regression problems. This algorithm is a variant of the Gradient Boosting framework and is an optimized tree learning algorithm that provides fast and effective learning. XGBoost offers the advantage of combining many base models to achieve powerful predictive power. Additionally, when used in conjunction with techniques such as feature selection and model tuning, it typically delivers high accuracy and performance. Therefore, XGBoost has a wide range of applications, from industrial applications to competitions, and is preferred for obtaining effective results even with large datasets [15]. The most general formula used in the XGBoost algorithm is given in equation 2.

$$F(x) = L(\theta) + \Omega(\theta) \tag{2}$$

In Equation 2, (x) represents the general function predicted by the model, $L(\theta)$ denotes the loss function on the data, and $\Omega(\theta)$ signifies the regularization term controlling the complexity of the model.

$$L(\theta) = \sum_{i=1}^{n} -(y_i \, log \, log \, (\hat{y}_i) \, + (1 - \, y_i) \, log \, log \, (\hat{y}_i) \,) \tag{3}$$

In Equation 3, it represents the cross-entropy loss used in a classification model. (θ) denotes the loss function calculated based on the model's parameters. y_i represents the true class label, while $\hat{y}_i$represents the probability value predicted by the model. The cross-entropy loss measures the difference between the true class label and the probability distribution predicted by the model for each data point. If the true class label is y_i, the loss function is computed as $(\hat{y}_i)$; otherwise, it is calculated as $(1 - \, y_i \,)$ These losses gauge how far off the model's prediction is from the true class label. The total loss is computed as the sum of these error terms across all data points.

$$\Omega(\theta) = \, \gamma T + \, \frac{\lambda}{2} \sum_{j=1}^{T} w_j^2 \tag{4}$$

In Equation 4, $\Omega(\theta)$ represents the regularization term, where γ and λ are regularization parameters. T denotes the number of trees in the ensemble, and w_j represents the weight assigned to the jth tree. The regularization term consists of two parts: The first part, γT, penalizes the complexity of the model by multiplying the number of trees by a regularization parameter γ. The second part, $\frac{\lambda}{2} \sum_{j=1}^{T} \quad w_j^2$, applies L2 regularization to the weights of the trees, where λ controls the strength of regularization. This regularization term helps prevent overfitting by discouraging overly complex models and promoting smoother solutions.

3.3.3 LightGBM

LightGBM is a machine learning algorithm that has gained popularity recently and is often preferred for fast and high-performance modeling on large datasets. This algorithm is a variant of the Gradient Boosting framework and has a structure that enables faster training times and lower memory usage. LightGBM is designed to model complex relationships using tree-based learning methods and is typically successful in dealing with large-scale datasets and high-dimensional feature spaces. Additionally, its ability to directly support categorical features and its parallel computation capabilities have made it a preferred choice for large-scale machine learning problems. Therefore, LightGBM is widely used in various applications, especially in industrial applications and large-scale data analysis projects [16].

$$F_m = \, F_{m-1}(x) + \, \eta \, \cdot \, h_m(x) \tag{5}$$

Equation 5 represents the update rule used in the LightGBM (Light Gradient Boosting Machine) algorithm. F_m represents the prediction of the model at the mmth iteration, while $F_{m-1}(x)$ is the prediction of the model from the previous iteration. η is the learning rate, and $h_m(x)$ is the candidate tree. In LightGBM, in each iteration, the weighted version of the candidate tree $h_m(x)$ is added to the prediction of the current model. This candidate tree is trained to focus on further reducing the residuals in the dataset, aiming to improve the performance of the model.

3.3.4 Random forest (RF)

Random Forest (RF) is a widely used algorithm in machine learning, often preferred for solving classification and regression problems. This algorithm is an ensemble of multiple decision trees that come together. Each decision tree is trained on randomly selected subsets of features and data points, resulting in independent predictions. These predictions are then combined by averaging them or by selecting the most common class or value. Random Forest is resilient to overfitting and typically provides high accuracy. Additionally, it can effectively scale to handle large-scale datasets due to its parallel computation capabilities. Therefore, Random Forest has a broad range of applications and is successfully used in many fields, from industrial problems to computational biology [17].

$$f(x) = \frac{1}{N}\sum_{i=1}^{N} f_i(x) \tag{6}$$

Equation 6 represents the fundamental prediction function used in the Random Forest (RF) algorithm. $f(x)$ denotes the prediction made for the input x. For each tree i, $f_i(x)$ represents the prediction of that tree. The overall prediction is obtained by averaging the predictions of all trees. In other words, $f(x)$ is the average of predictions from all trees for the data point x. This approach is a fundamental feature of the Random Forest algorithm, allowing for stronger and more generalizable predictions by combining predictions from multiple decision trees.

3.3.5 Support Vector Machine (SVM)

Support Vector Machine (SVM) is a powerful classification and regression algorithm widely used in the field of machine learning. This algorithm aims to find an optimized hyperplane to separate the data. SVM utilizes this hyperplane to determine the class of a particular data point, thereby achieving the widest possible margin between classes. Additionally, SVM provides flexibility through kernel functions, enabling it to handle both linearly separable and non-linearly separable datasets. Consequently, SVM is recognized as an effective tool for classifying complex datasets and often performs well in high-dimensional data spaces and with small datasets [17]-[18].

$$f(x) = w^T x + b \tag{7}$$

Equation 7 represents a linear decision boundary. $f(x)$denotes the predicted class for input feature vector x. w and b are the parameters to be learned by the model; w represents the weights associated with the feature vectors, and b is the bias term of the model.

$$margin = \frac{2}{\|w\|} \tag{8}$$

Equation 8 calculates the marginal distance around the decision boundary. $\|w\|$ represents the norm of the normal vector of the decision boundary (the magnitude of w).

$$minimize \ \frac{1}{2}\|w\|^2 \tag{9}$$

Equation 9 represents the loss function used during the training phase of SVM. The goal is to optimize the weights w used to determine the decision boundary. This equation is applicable for linearly separable classes.

$$K(x_i, x_j) = \phi(x_i)^T \phi(x_j) \tag{10}$$

Equation 10 represents the usage of kernel functions in SVM to enhance its flexibility. It denotes the inner product between two input vectors x_i and x_j Kernel functions transform data points from the input space to higher-dimensional spaces, making them linearly separable, especially when they are not linearly separable in the original input space.

3.3.6 K-Nearest Neighbors (KNN)

K-Nearest Neighbors (KNN) is a popular algorithm, especially for classification and regression tasks. This algorithm operates by calculating the distance between the input data point and neighboring points in the feature space. Subsequently, KNN determines the class or value of the input data point based on the classes or values of its nearest neighbors. The "k" in KNN represents the number of neighbors considered for classification or regression. KNN is a non-parametric algorithm as it does not make any assumptions about the underlying data distribution. Additionally, it is a versatile algorithm capable of handling both numerical and categorical data effectively. However, despite its simplicity and interpretability, KNN may face computational inefficiency with large datasets [18].

$$d(x_i, x_j) = \sqrt{\sum_{p=1}^{n} (x_{i,p} - x_{j,p})^2} \tag{11}$$

Equation 11 calculates the Euclidean distance between two data points x_i and x_j. $x_{i,p}$ and $x_{j,p}$ represent the feature values of the pth dimension of the data points.

$$y = mode(y_1, y_1, \dots, y_k) \tag{12}$$

Equation 12 represents the fundamental rule of the KNN algorithm for classification problems. To determine the class of a data point, the classes of its k nearest neighbors are collected, and the most frequently occurring class is assigned to the data point.

$$y = \frac{1}{k} \sum_{i=1}^{k} y_i \tag{13}$$

Equation 13 represents the fundamental rule of the KNN algorithm for regression problems. To determine the value of a data point, the values of its k nearest neighbors are collected, and the average of these values is used as the estimated value for this data point.

3.3.7 GRADİENT BOOSTİNG

Gradient Boosting is an effective ensemble learning technique widely used in machine learning. This technique enables the creation of a strong predictor by combining base models called weak learners. Gradient Boosting trains each base model to correct the errors of the previous model. This way, each successive model is improved to address the weaknesses of the previous models, thereby enhancing the overall prediction power. This process is optimized by carefully tuning hyperparameters such as the learning rate. Gradient Boosting yields successful results in various tasks, including classification and regression problems, and is commonly implemented with popular libraries such as XGBoost and LightGBM [19].

$$F_0(x) = 0 \tag{14}$$

Equation 14 represents the initial prediction of the Gradient Boosting algorithm. Initially, predictions start with zero.

$$F_m(x) = F_{m-1}(x) \; + \; \rho * h_m(x) \tag{15}$$

Equation 15 represents the fundamental update rule of the Gradient Boosting algorithm. $F_m(x)$ denotes the prediction at the mmth iteration, $F_{m-1}(x)$ represents the prediction from the previous iteration, $h_m(x)$ specifies the prediction function of the new model added in the mth iteration, and ρ indicates the contribution rate of the new model.

3.4 Explainable AI (XAI)

Explainable AI (XAI) is an approach aimed at making the decisions and inferences of artificial intelligence systems understandable and traceable by humans. XAI develops methods to explain the inner workings of complex AI models, allowing us to understand why decisions are made, how input data is processed, and how results are obtained. As a result, users can confidently accept the decisions of AI systems and question the logic behind them when necessary. XAI is recognized as an important tool for developing reliable and transparent AI systems in various fields, from medical diagnostics to financial risk analysis, autonomous vehicles, and security systems [20].

3.4.1 SHAP

SHAP (SHapley Additive exPlanations) is a technique used to explain predictions of complex artificial intelligence models. It particularly aids in understanding the inner workings of models like deep learning models, often referred to as black boxes, which are not easily interpretable. At the core of SHAP lies the concept of Shapley values from cooperative game theory. These values quantitatively measure the contribution of each feature to a prediction outcome. SHAP is utilized to understand the impact of each feature on a prediction outcome and visually elucidate the internal structure of the model. Consequently, it enhances the transparency of AI models' decisions and improves the model's reliability [21].

$$\phi_i(f) = \frac{1}{N!} \sum_{\pi} \left[f\left(x_{\pi(i)}\right) - f(x_\pi) \right] \tag{16}$$

Equation 16 represents a formula used in the SHAP (SHapley Additive exPlanations) algorithm. Here, $\phi_i(f)$ denotes the SHAP value of the ith feature of the model f. f represents the model's prediction function, N denotes the number of data points, x_π represents a permutation of π, and $x_{\pi(i)}$ represents the value of the ith feature in a permutation of π. This equation calculates the contribution of each feature to a prediction outcome as the SHAP value. This contribution is determined by averaging over all permutations. SHAP values quantify the impact of each feature on the model's predictions and make the model's decisions more interpretable.

3.4.2 LIME

LIME (Local Interpretable Model-agnostic Explanations) is a technique used to explain the decisions of complex artificial intelligence models. It particularly aids in understanding the behaviors of models termed as black boxes, whose internal workings are not fully understood. LIME is designed to interpret the predictions of these models locally. Its working principle is as follows: First, an example for which the prediction of the model to be explained is given. For instance, consider wanting to explain the prediction made by an image classification model for a specific image. LIME generates randomly perturbed examples around this example and evaluates the predictions of the model on these examples. Then, using the effects of these random examples on the model, LIME attempts to determine which features or variables determine the prediction. For example, to understand which pixels are most influential in the classification of an image, LIME analyzes the effects of the modified versions of pixels on the model prediction. Finally, the output of LIME is usually presented as a simple and understandable model. This model represents the local behavior of the original complex model and is easier to interpret. LIME is an effective tool used especially to make complex artificial intelligence models more understandable [22].

$$e(x) = \ argmin_{g \in \varsigma}(f, g, \pi_x) + \ \Omega(g) \tag{17}$$

Equation 17 represents a formula used in the LIME (Local Interpretable Model-agnostic Explanations) algorithm. Here, $e(x)$ denotes the best interpretable model for a specific data point x. The $argmin$ operator finds the minimum among all models g in a certain set ς, considering the smallest loss (f, g, π_x) and the complexity term $\Omega(g)$. This equation represents the process of finding the most suitable interpretable model for a specific data point in the LIME algorithm. LIME focuses on a small region around the data point to explain how the data point is influenced by the complex model, thereby enabling local interpretation of the model's decisions.

4 Results

In this study, various preprocessing steps have been applied to the dataset, with the main aim of enabling more effective utilization of categorical variables. Particularly, categorical variables in string format in the dataset have been converted to integer types to enhance the processing efficiency of models. This transformation process has included variables such as students' gender, age range, and parents' education level. These adjustments have facilitated better understanding of the dataset and yielded more accurate results. Additionally, the transformation has enabled algorithms working with numerical values to operate more effectively, leading to more reliable analysis outcomes. An example of the dataset used in the analysis is provided in Figure 2.

	school	sex	age	address	famsize	Pstatus	Medu	Fedu	Mjob	Fjob	...	romantic	famrel	freetime	goout	Dalc	Walc	health	absences	Lecture_Notes	Course_Pass_Status
0	0	0	18	0	1	1	4	4	0	4	...	0	4	3	4	1	1	3	6	28.333333	0
1	0	0	17	0	1	0	1	1	0	2	...	0	5	3	3	1	1	3	4	26.666667	0
2	0	0	15	0	0	0	1	1	0	2	...	0	4	3	2	2	3	3	10	41.666667	0
3	0	0	15	0	1	0	4	2	1	3	...	1	3	2	2	1	1	5	2	73.333333	1
4	0	0	16	0	1	0	3	3	2	2	...	0	4	3	2	1	2	5	4	43.333333	0
...	...	...	...	...	...	...	...	...	...	...	...	...	...	...	...	...	...	...	...	...	...
1039	1	0	19	1	1	0	2	3	3	2	...	0	5	4	2	1	2	5	4	51.666667	1
1040	1	0	18	0	0	0	3	1	4	3	...	0	4	3	4	1	1	1	4	76.666667	1
1041	1	0	18	0	1	0	1	1	2	2	...	0	1	1	1	1	1	5	6	53.333333	1
1042	1	1	17	0	0	0	3	1	3	3	...	0	2	4	5	3	4	2	6	50.000000	0
1043	1	1	18	1	0	0	3	2	3	2	...	0	4	4	1	3	4	5	4	53.333333	1

Figure 2 Dataset Example

The Biogeography-Based Optimization (BBO) algorithm has been effective in identifying complex relationships within the dataset and allowing the selection of attributes that are appropriate for the complexity among features. Therefore, the BBO algorithm is considered a suitable option in determining student success. In this study, using the BBO algorithm, the 20 attributes that most influence student success were identified from among the 32 attributes in the dataset.

With the determination of the most important 20 attributes using the BBo algorithm, these attributes were included in machine learning models, and metrics such as Accuracy, Precision, Recall, F1-score were used for their evaluation. The results of the evaluation conducted with the most important 20 attributes identified by the BBo algorithm are presented in Table 1 below.

Table 1: *The results of the evaluation conducted with the 20 most important attributes identified by the BBo algorithm*

Model	**Accuracy**	**Precision**	**Recall**	**F1-score**
Gradient Boosting*	0.7388	0.7311	0.7388	0.7234
Random Forest (RF)	0.7252	0.7414	0.7452	0.7290
XGBoost	0.7188	0.7317	0.7388	0.7313
LightGBM	0.7124	0.7244	0.7324	0.7220
K-Nearest Neighbors (KNN)	0.6815	0.6646	0.6815	0.6650
Support Vector Machine (SVM)	0.6514	0.6637	0.6624	0.5722
Artificial Neural Networks (ANN)	0.6624	0.6478	0.6624	0.6504

The confusion matrix of the Gradient Boosting algorithm with the highest Accuracy value is presented in Figure 3 based on the evaluation results obtained with the BBo algorithm using the most important 20 features.

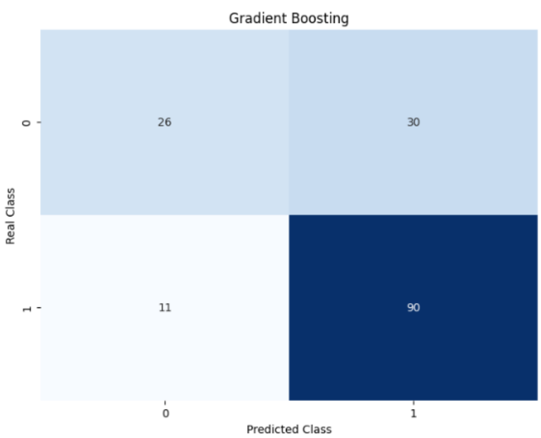

Figure 3 The output of the Gradient Boosting Confusion Matrix

- True Positive (TP): Represents the case where the model accurately predicts the positive class.
  TP = 90
- True Negative (TN): Represents the case where the model accurately predicts the negative class.
  TN = 11
- False Positive (FP): Represents the case where the model incorrectly predicts the positive class.
  FP = 30
- False Negative (FN): Represents the case where the model incorrectly predicts the negative class.
  FN = 26

The accuracy metric is a performance measure that evaluates the ratio of correctly predicted samples by a classification model. This metric is calculated based on True Positives (TP) and True Negatives (TN) values. A high accuracy value indicates that the model has a high ability to make correct predictions with few incorrect predictions. The accuracy metric is effective when all classes are correctly classified and can be used in balanced class distributions. However, in cases of imbalanced class distributions (for example, situations where there are rare classes), the accuracy metric may be inadequate because incorrect predictions of rare classes can misleadingly inflate the overall accuracy value. The calculation of the accuracy metric is shown in Equation 18.

$$Accuracy = \frac{TP + TN}{TP + TN + FP + FN} \tag{18}$$

The precision metric is a performance measure that evaluates how many of the samples predicted as positive by a classification model are actually positive. This metric is calculated based on the True Positive (TP) and False Positive (FP) values. A high precision value indicates that most of the samples predicted as positive are indeed positive, with few false positive predictions. The calculation of the precision metric is shown in Equation 19.

$$Precision = \frac{TP}{TP + FP} \tag{19}$$

The recall metric is a performance measure that evaluates how many of the true positives a classification model correctly predicts. This metric is calculated based on the True Positive (TP) and False Negative (FN) values. A high recall value indicates that the model correctly predicts most of the true positives, with few false negative predictions. The recall metric is particularly important in areas of vital importance, such as medical diagnosis, and in situations where missing true positives is significant. The calculation of the recall metric is shown in Equation 20.

$$Recall = \frac{TP}{TP + FN} \tag{20}$$

The F1 metric is the harmonic mean of a classification model's precision and recall metrics, aiming to balance the impact of both false positives and false negatives. This metric is calculated based on True Positive (TP), False Positive (FP), and False Negative (FN) values. A high F1 value indicates that both precision and recall metrics are high, and the model reduces both false positives and false negatives. The F1 metric is particularly useful in cases of imbalanced class distributions (for example, situations where there are rare classes), as precision and recall metrics may be inadequate in these scenarios. The calculation of the F1 metric is shown in Equation 21.

$$F1 = \frac{Precision \times Recall}{Precision + Recall} \tag{21}$$

The Gradient Boosting algorithm, which yielded the highest accuracy value, has been explained using interpretable artificial intelligence models SHAP and LIME. The explanations are provided in Figures 3 and 4.

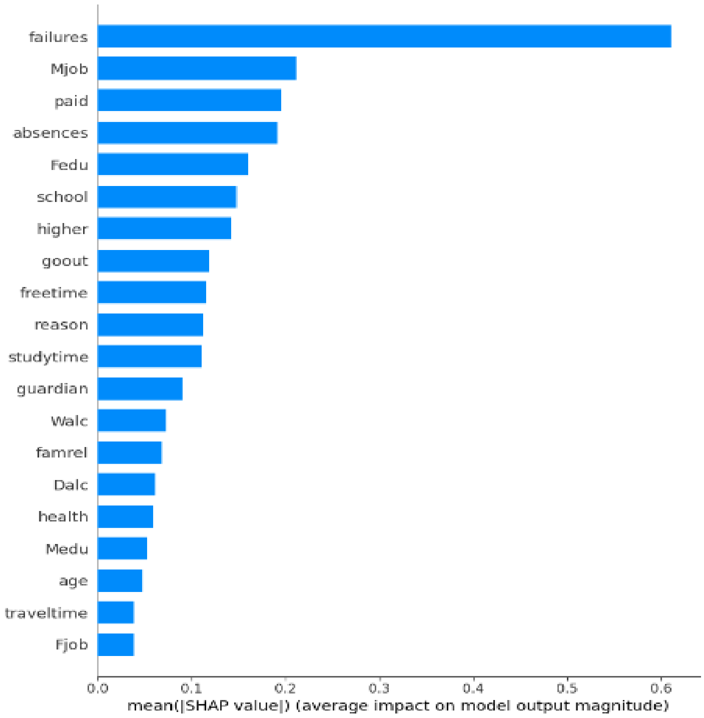

Figure 4 SHAP output, which is an explainable artificial intelligence model.

In Figure 4, a graph is presented illustrating the average effect size of a model's output and representing an explanation method that measures the individual contribution of each feature to the model's prediction using SHAP (SHapley Additive exPlanations) values. The graph displays the average absolute SHAP value on the x-axis and the average effect size on the y-axis. The features depicted in the graph include the number of 'failures', representing the instances of student failure, 'Mjob', indicating the mother's occupation, 'paid', denoting the student's employment status, and 'absences', representing the number of days the student has been absent from school. Among the conclusions that can be drawn from the graph, it is observed that the number of student failures and the mother's occupation have the greatest impact on the model's output, while the effects of other features are comparatively smaller. However, it is important to note that the graph may not fully represent the performance of the model for a specific student, and it is crucial to acknowledge that the effects of each feature are not linear and may not account for interactions between features.

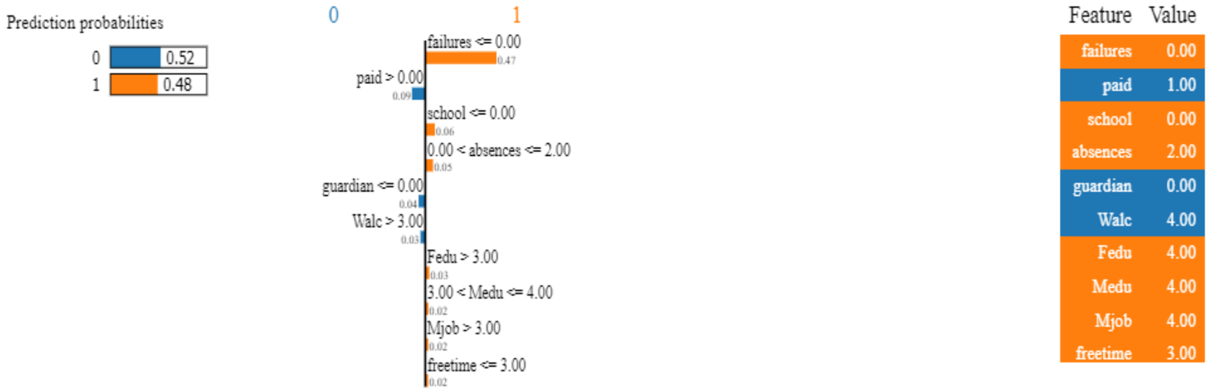

Figure 5 LIME output, which is an explainable artificial intelligence model.

Figure 5 contains information regarding student data and predictions made based on this data. The features include factors such as the number of failures, amount paid, type of school, number of absences, guardian status, test scores, and parental occupation. The effects of these features on the model prediction are explained using the LIME method, which demonstrates how the prediction changes with each feature value alteration. The graph highlights that the Walc, Fedu, and Medu test scores have the most significant impact on the model's prediction. This information indicates that these factors increase the likelihood of student success. However, it is also noted that other features contribute to the model's prediction, providing insights into how the prediction is generated. Thus, the LIME analysis serves as a valuable tool for educators and other stakeholders by making the model predictions more understandable.

5 Conclusions

The analyses conducted emphasize the necessity of examining the factors influencing student success in detail. Specifically, the discussion of how these factors impact learning outcomes is supported by theoretical frameworks. This study applied various preprocessing steps to the dataset, aiming to enable more effective utilization of categorical variables. Particularly, categorical variables in string format were converted to integer types, including variables such as students' gender, age range, and parents' education level. These adjustments facilitated better understanding of the dataset and yielded more accurate results, enhancing the processing efficiency of the models.

Furthermore, the evaluation of algorithms and interpretable artificial intelligence models used in determining student success demonstrates how data-driven decision-making processes in education can be shaped. The Biogeography-Based Optimization (BBO) algorithm was particularly effective in identifying complex relationships within the dataset, selecting the 20 most influential attributes from among the 32 attributes. This selection improved the performance of machine learning models, as evidenced by metrics such as Accuracy, Precision, Recall, and F1-score.

The results indicate that models like Gradient Boosting and Random Forest performed well, with Gradient Boosting achieving an accuracy of 0.7388 and Random Forest achieving an accuracy of 0.7252. These findings highlight the potential of advanced algorithms to provide reliable insights into student success.

Additionally, methods like SHAP (SHapley Additive exPlanations) and LIME (Local Interpretable Model-agnostic Explanations) were used to interpret the model predictions. The SHAP analysis revealed that features such as the number of failures and the mother's occupation had the greatest impact on the model's output. Similarly, LIME analysis indicated that factors like Walc, Fedu, and Medu test scores significantly influenced the model's predictions.

In light of these findings, there is a need for further research to create and implement education policies more effectively. Future studies should focus on deeper exploration of the factors influencing student success and better understanding the interactions among these factors. Additionally, there is a necessity to enhance the role of artificial intelligence techniques in education and integrate these techniques more effectively into educational practices.

The results of this study could contribute to the development of data-driven decision-making processes in education and more effectively planned interventions to improve student success. Moreover, this study serves as an important resource for educators and policymakers, aiding in the more sustainable and inclusive enhancement of the education system.

6 Declarations

6.1 Study Limitations

None.

6.2 Acknowledgement

The author would like to thank all the data sets, materials, information sharing and support used in the assembly of this article.

6.3 Funding source

The author gratefully acknowledge the financial support of Sakarya University of Applied Sciences AI And Data Science Research And Application Center.

6.4 Competing Interests

There is no conflict of interest in this study.

6.5 Author contributions

Cem Özkurt wrote and reviewed the article.

References

[1] Z. Akhtar, "Socio-economic status factors effecting the students achievement: a predictive study," *International Journal of Social Sciences and Education*, vol. 2, no. 1, pp. 281-287, 2012.

[2] Lakhan, G. R., Soomro, B. A., & Channa, A. (2021). INVESTIGATION OF THE SOCIO-ECONOMIC FACTORS THAT INFLUENCE YOUNG LEARNERS ACADEMIC SUCCESS: A CASE STUDY OF SECONDARY SCHOOLS OF SINDH, PAKISTAN. *New Horizons (1992-4399)*, 15(1).

[3] Marks, G. N. (2016). The relative effects of socio-economic, demographic, non-cognitive and cognitive influences on student achievement in Australia. *Learning and Individual Differences*, 49, 1-10.

[4] Singh, P., & Choudhary, G. (2015). Impact of socio-economic status on academic achievement of school students: An investigation. *International journal of applied research*, 1(4), 266-272.

[5] Albashish, D., Hammouri, A. I., Braik, M., Atwan, J., & Sahran, S. (2021). Binary biogeography-based optimization based SVM-RFE for feature selection. *Applied Soft Computing*, 101, 107026.

[6] Lau, E. T., Sun, L., & Yang, Q. (2019). Modelling, prediction and classification of student academic performance using artificial neural networks. *SN Applied Sciences*, 1(9), 982.

[7] Şahin, S., & Erol, Ç. (2024). Prediction of Secondary School Students' Academic Achievements with Machine Learning Methods and a Sample System. *Cybernetics and Systems*, 55(4), 940-960.

[8] Guleria, P., & Sood, M. (2023). Explainable AI and machine learning: performance evaluation and explainability of classifiers on educational data mining inspired career counseling. *Education and Information Technologies*, 28(1), 1081-1116.

[9] Alamri, R., & Alharbi, B. (2021). Explainable student performance prediction models: a systematic review. *IEEE Access*, 9, 33132-33143.

[10] Delen, D., Davazdahemami, B., & Rasouli Dezfouli, E. (2023). Predicting and mitigating freshmen student attrition: A local-explainable machine learning framework. *Information Systems Frontiers*, 1-22.

[11] Cruz-Jesus, F., Castelli, M., Oliveira, T., Mendes, R., Nunes, C., Sa-Velho, M., & Rosa-Louro, A. (2020). Using artificial intelligence methods to assess academic achievement in public high schools of a European Union country. *Heliyon*, 6(6).

[12] R. Hans and H. Kaur, "Hybrid Biogeography-Based Optimization and Genetic Algorithm for Feature Selection in Mammographic Breast Density Classification," *International Journal of Image and Graphics*, vol. 22, no. 03, p. 2140007, 2022.

[13] K. Bakshi and K. Bakshi, "Considerations for artificial intelligence and machine learning: Approaches and use cases," in *2018 IEEE Aerospace Conference*, 2018, pp. 1-9.

[14] Z. Zhang, "A gentle introduction to artificial neural networks," *Annals of translational medicine*, vol. 4, no. 19, 2016.

[15] X. Y. Liew, N. Hameed, and J. Clos, "An investigation of XGBoost-based algorithm for breast cancer classification," *Machine Learning with Applications*, vol. 6, p. 100154, 2021.

[16] A. Villar and C. R. V. de Andrade, "Supervised machine learning algorithms for predicting student dropout and academic success: a comparative study," *Discover Artificial Intelligence*, vol. 4, no. 1, pp. 1-24, 2024.

[17] L. H. Alamri, R. S. Almuslim, M. S. Alotibi, D. K. Alkadi, I. Ullah Khan, and N. Aslam, "Predicting student academic performance using support vector machine and random forest," in *Proceedings of the 2020 3rd International Conference on Education Technology Management*, December 2020, pp. 100-107.

[18] H. Al-Shehri, A. Al-Qarni, L. Al-Saati, A. Batoaq, H. Badukhen, S. Alrashed, J. Alhiyafi, and S. O. Olatunji, "Student performance prediction using Support Vector Machine and K-Nearest Neighbor," in *2017 IEEE 30th Canadian Conference on Electrical and Computer Engineering (CCECE)*, 2017, pp. 1-4. doi: 10.1109/CCECE.2017.7946847.

[19] C. Bentéjac, A. Csörgő, and G. Martínez-Muñoz, "A comparative analysis of gradient boosting algorithms," *Artificial Intelligence Review*, vol. 54, pp. 1937-1967, 2021.

[20] A. Adadi and M. Berrada, "Peeking Inside the Black-Box: A Survey on Explainable Artificial Intelligence (XAI)," *IEEE Access*, vol. 6, pp. 52138-52160, 2018. doi: 10.1109/ACCESS.2018.2870052.

[21] I. U. Ekanayake, D. P. P. Meddage, and U. Rathnayake, "A novel approach to explain the black-box nature of machine learning in compressive strength predictions of concrete using Shapley additive explanations (SHAP)," *Case Studies in Construction Materials*, vol. 16, p. e01059, 2022.

[22] K. R. Chowdhury, A. Sil, and S. R. Shukla, "Explaining a black-box sentiment analysis model with local interpretable model diagnostics explanation (LIME)," in *Advances in Computing and Data Sciences: 5th International Conference, ICACDS 2021, Nashik, India, April 23–24, 2021, Revised Selected Papers, Part I*, vol. 5, pp. 90-101, Springer International Publishing, 2021.

Review Paper
Journal of Smart Systems Research (JOINSSR) 5(1), 55-65, 2024
Received: 30-May-2024 Accepted: 20-June-2024
DOI: 10.58769/joinssr.1492524

Advancements and Innovations in Elbow Orthoses: An Extensive Review of Design, Development, and Clinical Applications

Hamid ASADI DERESHGI[1*], Sezer BICER[1], Ozge Naz GURBUZ[1], Dilan DEMIR[2]

[1]Department of Biomedical Engineering, Istanbul Arel University, hamidasadi@arel.edu.tr
[2]Artificial Intelligence Studies, Application and Research Center (ArelMED-I), Istanbul Arel University,

ABSTRACT

There are different types of elbow orthoses, medical devices engineered to support and stabilize the elbow joint, assisting in recovery from injuries or surgeries, and managing chronic conditions through movement restriction and essential immobilization. The development of elbow orthoses has evolved significantly from rudimentary splints in early medical practices to advanced, custom-fitted devices utilizing modern materials and biomechanical principles. This review provided researchers with a comprehensive overview of the history and development of elbow orthoses. It offered insights into the effectiveness, utilization, and clinical applications of different types of elbow orthotic designs. Additionally, this review contributed to the body of knowledge by comparing traditional and modern elbow orthotic technologies, offering valuable guidance for future research directions in this area of study. Furthermore, this review underscored the challenges and prospects within the field, paving the way for concerted endeavors among academics, healthcare practitioners, and industrial experts to propel the development of elbow orthotic technologies and improve patient results. Thus, researchers potentially could have developed more effective treatment strategies in clinical practice and improved the quality of life for patients.

Keywords: Elbow orthoses, rehabilitation, biomechanics, personalized medicine

1 Introduction

The elbow joint, or articulatio cubiti, is a complex synovial hinge joint comprising the distal humerus, proximal ulna, and head of the Radius [1]. It includes three primary articulations known as the humeroulnar, humeroradial, and proximal radioulnar joints, which facilitate flexion, extension, pronation, and supination [2]. Stability is provided by the medial and lateral collateral ligaments as well as the annular ligament [3]. The surrounding musculature, including the biceps brachii, brachialis, and triceps brachii, supports joint function and stability [4]. The proximity of critical neurovascular structures, including the ulnar, radial, and median nerves, along with the brachial artery, necessitates a thorough understanding of elbow anatomy for accurate clinical assessment and intervention [5]. There are numerous elbow injuries and disorders, including lateral epicondylitis, medial epicondylitis, olecranon bursitis, cubital tunnel syndrome, and ligamentous injuries, that frequently occur and require precise and effective rehabilitation protocols [6]. The primary goals of elbow rehabilitation encompass pain management, reduction of inflammation, and restoration of functional mobility and strength [7-9]. Conventional therapeutic protocols encompass manual therapy, specific therapeutic exercises, cryotherapy, and neuromuscular electrical stimulation [10]. The implementation of elbow orthoses stands

[*] Corresponding Author's email: hamidasadi@arel.edu.tr

out as a crucial intervention in the management of these conditions [11]. Orthoses provide crucial joint stabilization, mitigate pain, and facilitate controlled mobilization, thereby enhancing the healing process [12]. By restricting deleterious movements and reducing mechanical stress on the affected structures, orthoses not only promote tissue recovery but also prevent recurrence of injury, making them an indispensable component of a comprehensive rehabilitation strategy for elbow disorders [13].

Elbow orthoses, encompassing passive, active, and semi-active modalities, are extensively utilized in the treatment and management of a spectrum of conditions including epicondylitis, elbow instability, fractures, and traumatic injuries [14-15]. Passive orthoses typically offer stable support, allowing the elbow to rest comfortably [16]. Active orthoses promote elbow motion alongside restricting excessive movement [17]. Semi-active orthoses facilitate a specific range of motion, enabling users to engage muscle strength and movement [18]. The working principles of these orthoses are to stabilize the elbow in accordance with biomechanical principles, restrict undesirable movements, and apply pressure to the affected site [19]. These designs are typically made from lightweight and durable materials such as titanium [20], aluminum [21], or carbon fiber [22] and can be adjusted according to individual needs.

Elbow orthoses, initially introduced in the medical field in the early twentieth century, found their earliest applications in the management of conditions such as epicondylitis and elbow fractures [23]. The historical evolution of elbow orthoses has been marked by advancements in mechanical design, structural composition, and manufacturing processes [24]. Early orthoses were often rudimentary, consisting of simple splints or braces constructed from materials such as metal or leather [25]. Over time, innovations in materials science led to the development of lighter, more durable orthotic materials, including plastics, carbon fiber [27], and thermoplastics [28]. Concurrently, improvements in biomechanical understanding and orthotic design principles have enhanced the effectiveness and comfort of elbow orthoses [28]. Today, elbow orthoses remain a crucial component of conservative treatment strategies for a range of elbow pathologies, offering targeted support [30-31], stability [32], and pain relief [33] to patients.

The purpose of this review paper was to provide a comprehensive synthesis of the existing literature concerning elbow orthoses. It delved into various aspects including their typologies, indications, applications, and efficacy in managing a spectrum of elbow pathologies such as epicondylitis, instability, fractures, and traumatic injuries. Furthermore, it scrutinized the biomechanical underpinnings of orthotic design, the materials utilized in orthosis fabrication, and technological advancements in the field. Through an exhaustive analysis and synthesis of prior research, this review paper contributed to the academic discourse by elucidating evidence-based practices in elbow orthotic management and identifying avenues for future research and innovation. The necessity for a review paper on elbow orthoses arises from the increasing prevalence of elbow-related injuries and conditions and the need for a comprehensive understanding of the efficacy and applications of orthotic interventions in their management. The structure of the paper was delineated as follows. In Section 2, the focus was on the development and advancements in dynamic elbow orthoses, showcasing innovative designs and technological features intended to improve functional results and rehabilitation processes. Finally, a thorough review of the concluding remarks was conducted in Section 3.

2 Orthotic Innovations in Elbow Rehabilitation

In recent years, significant advancements have been achieved in the design and application of elbow orthoses for various clinical conditions. These devices have evolved to provide enhanced support, stability, and therapeutic benefits, utilizing innovative technologies and materials. This section provides a concise overview of notable studies and developments in the field of elbow orthoses, highlighting their clinical implications and technological advancements. There is an extensive collection of studies available in the open literature. Figure 1 illustrates the number of academic publications indexed by Web of Science (WoS) between 1980 and 2023. This review paper highlights several studies noted for their innovative contributions (see Figure 2). For example; Deharde and Patchel (1997) developed a dynamic splint incorporating a bi-directional torsional power unit for extension or flexion support, featuring adjustable force, compactness, and lightweight design. This invention utilized a hinge-mounted power unit to selectively oppose joint movement, with self-aligning contour plates ensuring anatomical conformity and stability. Innovative features encompassed a universal soft cuff/strap design, infinitely adjustable telescoping struts, and a cam locking mechanism for secure positioning [34]. Johnson et al. (2001) developed the Motorized Upper-Limb Orthotic System as an advanced powered orthosis designed for individuals with disabilities or limb weakness. It featured five degrees of freedom focusing on shoulder, elbow, and pronation/supination movements. The system operated in assistive, continuous passive motion therapy, and potential exercise modes, demonstrating capability in providing controlled movements and effective therapy programming, with attention to safety considerations for future enhancements in operation and control interfaces [35]. Bahadir et al. (2005) conducted a study to investigate the effect of using the Bobath sling on glenohumeral subluxation and functional improvement in hemiplegic patients. A total of 32 hemiplegic patients with an average age of 58.7 were included in the study. The comparison between patients using the Bobath sling and those not using it revealed that after one month of treatment, patients using the Bobath sling experienced a decrease in glenohumeral subluxation or stability without progression. These findings indicated that the use of the Bobath sling could be beneficial in preventing the development and progression of glenohumeral subluxation in hemiplegic patients [36]. Vanderniepen et al. (2008) discussed the design challenges and unique characteristics of orthopaedic rehabilitation for the elbow joint using a powered orthosis with MACCEPA actuators. The paper highlighted the differences in approaches between neuro-rehabilitation and orthopaedic rehabilitation, emphasizing the specific considerations needed for effective elbow joint rehabilitation. Additionally, the paper detailed the mechanical design and requirements of the orthosis, particularly focusing on the innovative features of MACCEPA actuators with online adaptable compliance [37]. Schulz et al. (2009) developed a non-invasive, modular FES-hybrid orthosis for upper extremity rehabilitation in cervical spinal cord injured patients. This orthosis integrated orthotic stability with FES muscle activation to restore function and enable training. By using miniaturized flexible fluidic actuators and innovative user interfaces based on muscle activity and movement intention detection, the system aimed to address grasping function loss, enhancing independence and autonomy for patients [38]. Kesmezacar et al. (2010) conducted a study to investigate the clinical and radiographic outcomes of conservatively managed simple elbow dislocations. Patients treated with closed reduction and short-term immobilization exhibited notable restrictions in joint range of motion, and most patients did not report feeling fully healed. These findings suggested a correlation between significant joint mobility limitations and the treatment approach for simple elbow dislocations, despite the effectiveness of these methods in terms of functional scores [39].

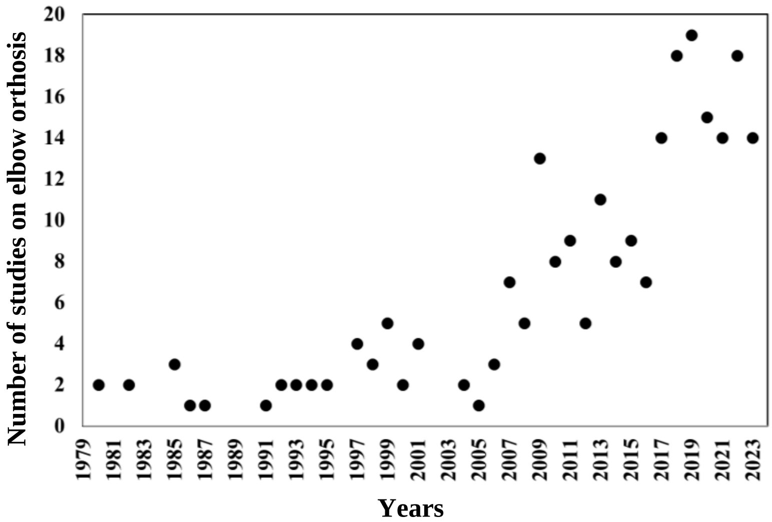

Figure 1: Academic publication trends on elbow orthosis in web of science

Figure 2: Compilation of elbow orthosis designs from reviewed studies

Pau et al. (2012) developed a neuromuscular interface (NI) for the elbow joint that predicts motion using electromyographic (EMG) signals from the biceps and triceps. The study demonstrated that the NI, which did not rely on additional weights or other sensors, achieved an average root-mean-square error of 6.53° for single cycles and 22.4° for random cycles, validating its potential for both able-bodied and less-abled users [40]. Bonutti et al. (2012) conducted a patent study and devised an orthosis that enabled hand and arm bone movement. The orthosis included a main gear assembly with a lower cuff for wrist and hand grip, allowing adjustments for pronation and supination. A lower cuff arm stabilized the forearm, and an upper cuff arm supported the upper arm, accommodating angular adjustments for personalized therapy sessions [41]. Cempini et al. (2013) introduced enhancements to the NEUROExos, a wearable exoskeleton designed for mobilizing paretic/spastic elbows. The study focused on the exoskeleton's actuation, transmission, and control systems, incorporating a safety clutch and a series elastic actuation architecture with a novel torsional spring element to improve joint compliance and enable both position and torque control methods. The revised NEUROExos was designed to be portable and accessible for clinical application [42]. Ripel et al. (2014) designed a motorized active elbow orthosis (AEO) for rehabilitation, utilizing robotic exoskeleton principles. The device measures patient motion using a strain gauge and controls the actuator to aid elbow movement, offering exercises similar to those of a physiotherapist. Initial tests demonstrated successful improvement in elbow joint motion, suggesting potential for home-based rehabilitation with further validation needed for widespread clinical adoption [43]. Vitiello et al. (2016) developed an advanced version of the NEUROExos robotic elbow exoskeleton, targeting rehabilitation for stroke patients in both acute and subacute phases. This version introduced a novel series elastic actuation system, an anatomical alignment mechanism with four passive degrees of freedom, and one active degree of freedom with remote cable-driven actuation. Initial trials with chronic post-stroke patients indicated the system's effectiveness in assessing joint rigidity and its potential for rehabilitation application [44]. Herrnstadt et al. (2016) designed a one DOF elbow orthosis for tremor suppression, utilizing a speed-controlled, voluntary-driven approach. In contrast to traditional methods that canceled tremor signals, this orthosis estimated and actuated based on voluntary movement, achieving over 99% reduction in tremor power with minimal impact on voluntary motion. The feasibility of this approach was demonstrated through testing with a robotic system that simulated the human arm [45]. Ataoğlu et al. (2017) evaluated the efficacy of closed reduction followed by early mobilization in patients with simple elbow dislocations. The study included 18 adults treated with closed reduction under sedation, followed by a week of immobilization in a long arm cast and early active movement initiation. After one year, evaluations using the Quick Disabilities of the Arm, Shoulder, and Hand (Quick-DASH) and Oxford Elbow Score showed no significant differences compared to the contralateral elbow. Early mobilization resulted in quicker return to work and no recurrent dislocations, demonstrating its safety and effectiveness [46]. Cilaci et al. (2018) documented the rehabilitation process of a 33-year-old woman with localized scleroderma, focusing on severe joint contractures in her left upper extremity. The therapy had included heated modalities, active stretching and strengthening exercises, and the use of a dynamic orthosis. Over one month, improvements were noted in range of motion, particularly elbow extension and shoulder abduction, with a significant increase in grip strength and improved DASH scores. These findings highlighted the effectiveness of conventional rehabilitation methods augmented by dynamic orthoses in treating rigid contractures in localized scleroderma [47]. Murugan et al. (2018) developed an ergonomic elbow orthosis to address elbow hyperextension, utilizing a 3D scanned model of the human hand for a personalized design. The orthosis, constructed from ABS material through additive manufacturing, was optimized for weight and stiffness, ensuring comfort and faster recovery compared to conventional methods [48]. Wee et al. (2019) developed an elbow-flexion assist orthosis for individuals with arthrogryposis multiplex congenita (AMC), aiming to aid elbow flexion using a spring mechanism combined with a sliding joint to increase elbow torque. The prototype demonstrated increased elbow flexion from 87 degrees without the device to 120 degrees with it, allowing the user to bring her hand to her mouth more easily. This lightweight, easily concealable orthosis offered a practical solution for enhancing elbow movement in AMC patients [49]. Bancud et al. (2019) designed a powered wearable orthosis for managing spasticity and contractures resulting from neurological and orthopedic pathologies. This portable device enabled patients to perform repeated-passive-dynamic exercises in non-clinical environments. Equipped with electrogoniometers and torque sensors, the orthosis recorded kinematic and dynamic data, providing valuable insights for clinicians and supporting further research. The modular design allowed adaptability to various anatomies and conditions, addressing limitations of existing robotic rehabilitation devices [50]. Minh et al. (2019) developed a low-cost, mechatronic orthosis for home-based rehabilitation of elbow injuries, which used EMG sensors to detect and translate muscle signals into motor movements. The device, regulated for various users, utilized adaptive control algorithms including linear quadratic Gaussian and Kalman filter to achieve a 94% accuracy, with a maximum error of 6.9° over a 122° movement range [51]. Dindorf and Wos (2019) developed a wearable elbow joint orthosis featuring a bimuscular pneumatic servo-drive controlled by bioelectric signals. The study presented the use of brain activity and muscle tension to manage the orthosis, utilizing a distributed control system with a master and direct layer. The orthosis facilitated natural elbow movements and provided effective support for rehabilitation and muscle force recovery [52]. Bonutti et al. (2019) introduced a novel invention, a patented orthosis aimed at facilitating supination and/or pronation of the wearer's forearm. The orthosis consisted of a base, an upper arm support securing the wearer's upper arm, a rotation assembly enabling rotation within a defined plane, and a forearm support engaging the wearer's wrist and forearm. This innovation aimed to provide effective support for forearm rotation, enhancing rehabilitation and mobility for individuals [53]. Nikolaev et al. (2020) aimed to develop an adaptive elbow orthosis allowing for customizable motor activity engagement and remote control. The proposed design included individual sockets for the shoulder and forearm, elastic elements for torque balance, adaptation drives, and a control system operated via an Android mobile app with feedback [54]. Golovin et al. (2021) investigated a new orthosis design for patients with upper limb paresis, addressing the limitations of existing devices. Their prototype, combining elastic elements and external energy sources, enabled precise control of auxiliary force via a smartphone application, potentially enhancing rehabilitation effectiveness [55]. Demirsoy et al. (2022) developed a Raspberry Pi-controlled remote monitoring system. This system utilized EMG signals, storing the data in the cloud for access by physiotherapists. The study introduced a low-cost, portable, and lightweight elbow rehabilitation device prototype. This device could be used for the treatment of nerve and tendon injuries, supporting active exercises, and enabling physiotherapists to monitor the rehabilitation progress [56]. Rodriguez et al. (2022) designed and simulated a 3 DOF mechatronic orthosis to support physical rehabilitation for individuals with musculoskeletal disabilities. The orthosis, tested on a 22-year-old subject, utilized 6061 aluminum rods, servomotors, and an Arduino Nano for control, along with a Matlab GUI for customization. Simulation results indicated that the orthosis achieved the desired angular movements for shoulder, arm, and elbow, showing potential for effective home-based rehabilitation [57]. Lavrenko et al. (2022) developed a prototype orthosis for elbow joint rehabilitation, focusing on stress-strain analysis and material selection for structural elements. The orthosis design incorporated a bevel gear mechanism, ensuring proper torque transmission, and was tested using FEMAP with NASTRAN to optimize its mechanical performance. The prototype demonstrated potential for post-traumatic rehabilitation and could be adapted for other joints [58]. Rosero et al. (2022) designed a mechatronic orthosis to aid elbow rehabilitation by facilitating flexion-extension and pronation-supination movements. Evaluated in practical applications, the device demonstrated potential as a low-cost, functional prototype for treating elbow pathologies, despite some identified design limitations and areas for improvement [59]. Said et al. (2022) purposed a smart elbow brace (SEB) designed for home-based rehabilitation of poststroke or traumatic elbow injuries. The SEB aimed to reduce elbow stiffness by facilitating extension, flexion, pronation, and supination motions. It incorporated a sliding joint to distribute forces and featured rehabilitation exercises for interactive engagement. However, clinical efficacy and signal delays remained as limitations, suggesting areas for future improvement [60]. Petrov et al. (2023) developed an autonomous controller for an active elbow orthosis, enabling parameterization by physiotherapists and independent use by patients at home. The controller operated in two modes, either without electromyographic feedback or using feedback from the biceps brachii muscle to initiate movement. The prototype was designed for both left and right elbows and included adjustable length options for different patient sizes [61]. In examining studies presented in the open literature, evidence suggested that elbow orthoses experienced significant advancements by incorporating modern technologies to provide superior support and therapeutic benefits. The ongoing development in this field had the potential to further refine and innovate, thus shaping the future of orthopedic rehabilitation. Section 3 summarized the main results of the studies on elbow orthoses.

3 Conclusions

The development of elbow orthoses was profoundly influenced by advancements in materials, design methodologies, and technological breakthroughs. These innovations drove a transformative shift in orthopedic rehabilitation, underscoring the remarkable progress and potential within the realm of elbow orthoses. The primary focus of elbow orthoses was to provide support, stability, and pain relief, with recent developments expanding their therapeutic potential to include dynamic rehabilitation, personalized intervention, and remote monitoring capabilities. One notable trend in recent research was the integration of advanced technologies into orthotic design, such as EMG sensors, mechatronic actuators, and adaptive control systems. These innovations enabled orthoses to respond dynamically to the patient's physiological signals, providing tailored support and facilitating more natural movement patterns during rehabilitation. Additionally, the incorporation of remote monitoring features allowed for real-time assessment of patient progress and adjustment of treatment protocols, enhancing the efficiency and effectiveness of rehabilitation interventions. Moreover, the emphasis on personalized medicine spurred the development of custom orthotic solutions tailored to individual patient anatomy and pathology. The application of 3D scanning and additive manufacturing technologies enabled the precise fabrication of orthoses tailored to the unique biomechanical requirements of patients, thereby optimizing comfort, fit, and therapeutic results. This personalized method not only enhanced patient adherence and satisfaction but also maximized the therapeutic efficacy of orthotic interventions. Furthermore, the expansion of orthotic applications beyond traditional rehabilitation centers was evident in recent research endeavors. The integration of elbow orthoses into patients' daily activities extended beyond clinical settings, ranging from home-based rehabilitation systems to assistive devices. This trend exemplified a broader paradigm shift towards patient-centered care and empowerment, wherein individuals were actively involved in the management of their health and well-being.

However, several challenges and limitations persist in the field of elbow orthoses. First, the high cost of advanced orthotic devices poses a significant barrier, limiting accessibility, particularly in low- and middle-income countries. Second, the effective utilization of these sophisticated technologies requires specialized training for both clinicians and patients, potentially hindering optimal use and reducing therapeutic benefits. Third, there is an insufficiency of comprehensive long-term studies evaluating the efficacy and reliability of these devices, making it difficult to draw definitive conclusions about their long-term benefits and potential complications. Fourth, the customization process for personalized orthoses faces biomechanical design challenges, as the unique anatomical and biomechanical characteristics of each patient require highly individualized solutions. Finally, the integration of smart technologies raises concerns about data security and patient privacy, necessitating robust measures to protect sensitive health information. Addressing these challenges through continued research and interdisciplinary collaboration will be essential for further advancement in the field. In light of the significant global health ramifications, it becomes imperative to prioritize the resolution of these challenges to facilitate equitable access to orthotic solutions on a global scale.

In conclusion, the field of elbow orthoses witnessed significant advancements towards personalized, technology-driven rehabilitation solutions that extended beyond conventional limits. Despite significant advancements in the design and application of elbow orthoses, several knowledge gaps remain. Future research should focus on the long-term efficacy of orthoses, enhancing personalization through advanced materials and AI-driven customization, and integrating smart technologies for real-time data collection and feedback. Additionally, optimizing biomechanical design and conducting comprehensive clinical trials will be crucial. Furthermore, the development of standardized protocols for training and data management can enhance the integration and efficacy of these devices. As research continued to push the boundaries of innovation, the future held promise for even more sophisticated orthotic interventions that improved patient benefits, promoted independence, and enhanced the quality of life for individuals with elbow-related conditions. In closing, the trajectory of elbow orthoses exemplifies a remarkable fusion of innovation and patient-centered ethos, offering a glimpse into a future wherein rehabilitation is not only effective but also seamlessly tailored to individual needs, ushering in a new era of orthopedic care.

4 Declarations

4.1 Study Limitations

None.

4.2 Acknowledgements

Special thanks to the ArelMED-I members for their motivations, recommendations and feedback.

4.3 Funding Source

This review was supported by the Research Fund of Istanbul Arel University (Project Number: 2022-ST-002), which significantly contributed to the successful completion of this study.

4.4 Competing Interests

The authors declare that they have no known competing financial interests or personal relationships that could have appeared to influence the work reported in this paper.

4.5 Authors' Contributions

Hamid ASADI DERESHGI provided supervision and guidance throughout the review process, ensuring the methodological rigor and integrity of the study. He participated in the conceptualization and design of the review, critically reviewed and revised the manuscript, and provided valuable intellectual contributions. He offered expertise in the field of elbow orthoses and contributed to the final approval of the manuscript.

Sezer BICER assisted in the conception and design of the review study, contributed to the selection and screening of relevant literature, and provided critical revisions to the manuscript for important intellectual content. He played a key role in synthesizing the information from the reviewed papers and ensuring the coherence of the narrative.

Ozge Naz GURBUZ contributed to the critical evaluation and synthesis of the reviewed literature, ensuring the accuracy and integrity of the information presented.

Dilan DEMIR contributed to the data collection process by identifying and retrieving relevant papers, and contributed to the development of figures included in the manuscript.

References

[1] Standring, S., Ellis, H., Healy, J., Johnson, D., Williams, A., Collins, P., & Wigley, C. (2005). Gray's anatomy: the anatomical basis of clinical practice. *American journal of neuroradiology*, 26(10), 2703.

[2] Moore, K. L., Dalley, A. F., & Agur, A. M. (2013). *Clinically oriented anatomy*. Lippincott Williams & Wilkins.

[3] Morrey, B. F. (2009). The elbow and its disorders. Elsevier Health Sciences.

[4] Fam, A. G., Lawry, G. V., & Kreder, H. J. (2006). *Musculoskeletal examination and joint injection techniques*. Mosby.

[5] Cleland, J., Koppenhaver, S., & Su, J. (2015). *Netter's orthopaedic clinical examination: an evidence-based approach*. Elsevier Health Sciences.

[6] Skirven, T. M., Osterman, A. L., Fedorczyk, J., Amadio, P. C., Felder, S., & Shin, E. K. (2020). *Rehabilitation of the hand and upper extremity*. Elsevier Health Sciences.

[7] Wilk, K. E., & Arrigo, C. (1993). Current concepts in the rehabilitation of the athletic shoulder. *Journal of Orthopaedic & Sports Physical Therapy*, 18(1), 365-378.

[8] Donatelli, R. A., & Wooden, M. J. (2009). *Orthopaedic physical therapy*. Elsevier health sciences.

[9] Di Giacomo, S., Kantar, S. S., Rotini, R., & Porcellini, G. (2018). *The Elbow: Principles of Surgical Treatment and Rehabilitation*. Springer.

[10] Cameron, M. H. (2021). *Physical agents in rehabilitation: An evidence-based approach to practice*. Elsevier Health Sciences.

[11] Jacobs, M. A., Austin, N. M., & Austin, N. M. (2013). *Orthotic intervention for the hand and upper extremity: splinting principles and process*. Lippincott Williams & Wilkins.

[12] Chui, K. K. (2020). *Orthotics and prosthetics in Rehabilitation*. Elsevier.

[13] Placzek, J. D., & Boyce, D. A. (2006). *Orthopaedic physical therapy secrets - E-book*. Hanley & Belfus.

[14] Asadi Dereshgi, H., Dal, H., Demir, D., & Türe, N. F. (2021). Orthoses: A Systematic Review. *Journal of Smart Systems Research*, 2(2), 135-149.

[15] da Silva, J. L. G. F., Gonçalves, S. M. B., da Silva, H. H. P., & da Silva, M. P. T. (2022). Three-dimensional printed exoskeletons and orthoses for the upper limb—A systematic review. *Prosthetics and Orthotics International*, 10-1097.

[16] Chen, B., Lin, J., Liu, L., & Niu, W. (2017). Static progressive orthoses for elbow contracture: a systematic review. *Journal of Healthcare Engineering*, 2017.

[17] Yasukawa, A., Lulinski, J., Thornton, L., & Jaudes, P. (2008). Improving elbow and wrist range of motion using a dynamic and static combination orthosis. *JPO: Journal of Prosthetics and Orthotics*, 20(2), 41-48.

[18] Zahedi, A., Wang, Y., Martinez-Hernandez, U., & Zhang, D. (2021). A wearable elbow exoskeleton for tremor suppression equipped with rotational semi-active actuator. *Mechanical Systems and Signal Processing*, 157, 107674.

[19] Mo, J., & Priefer, R. (2021). Medical devices for tremor suppression: current status and future directions. *Biosensors*, 11(4), 99.

[20] Viscuso, S., Pittaccio, S., Caimmi, M., Gasperini, G., Pirovano, S., Villa, E., ... & Molteni, F. (2009). Pseudoelastic nitinol-based device for relaxation of spastic elbow in stroke patients. *Journal of materials engineering and performance*, 18, 805-813.

[21] Huamanchahua, D., Castañeda-Vásquez, C., Vásquez-Espinoza, A., & Muñoz-Zevallos, A. (2021, December). Robotic Devices Types Exoskeletons for Elbow Rehabilitation: A Technological Review. *In 2021 IEEE 12th Annual Ubiquitous Computing, Electronics & Mobile Communication Conference (UEMCON)* (pp. 0791-0796). IEEE.

[22] Ameen, S. H. (2016). Manufacturing and numerical analysis of elbow orthosis made of polypropylene–carbon fiber–polypropylene. *Journal of Engineering and Sustainable Development*, 20(4), 186-199.

[23] Webster, J. B., & Murphy, D. P. (2017). *Atlas of Orthoses and Assistive Devices E-Book*. Elsevier Health Sciences.

[24] Kempfer, J., Lewis, R., Fiedler, G., & Silver-Thorn, B. (2022). Prosthetic and orthotic devices. *Rehabilitation Engineering: Principles and Practice*.

[25] Humans, J. M., Postema, K., & Geertzen, J. H. B. (2004). Elbow orthoses: a review of literature. *Prosthetics and orthotics international*, 28(3), 263-272.

[26] Gallucci, G. L., Boretto, J. G., Dávalos, M. A., Alfie, V. A., Donndorff, A., & De Carli, P. (2014). The use of dynamic orthoses in the treatment of the stiff elbow. *European Journal of Orthopaedic Surgery & Traumatology*, 24, 1395-1400.

[27] Wiegand, R., Schmitz, B., Pylatiuk, C., & Schulz, S. (2011). Mechanical performance of actuators in an active orthosis for the upper extremities. *Journal of Robotics*, 2011.

[28] Chinchalkar, S. J., Pearce, J., & Athwal, G. S. (2009). Static progressive versus three-point elbow extension splinting: a mathematical analysis. *Journal of Hand Therapy*, 22(1), 37-43.

[29] Mariscal, G., & Barrios, C. (2024). Assessing Biomechanical and Clinical Outcomes of an Elbow Orthosis Intervention in Youth Baseball: Preliminary Results. *Sports*, 12(1), 24.

[30] Ganesan, S., & Ranganathan, R. (2023). Design and development of customized elbow orthosis using additive manufacturing. *Proceedings of the Institution of Mechanical Engineers, Part L: Journal of Materials: Design and Applications*, 237(8), 1836-1846.

[31] Kacmaz, K. S., & Unver, B. (2024). Immediate effects of elbow orthoses on elbow proprioception in asymptomatic individuals: A randomized sham-controlled single-blinded study. *Journal of Hand Therapy*.

[32] Badre, A., Axford, D. T., Kotzer, S., Johnson, J. A., & King, G. J. (2024). Stabilizing effect of an elbow orthosis with an adjustable hinge axis after lateral collateral ligament injury: A biomechanical study. *Shoulder & Elbow*, 16(2), 193-199.

[33] Cavalcanti, A. M. G., Oliveira Filho, R. S. D., Gomes, H. C., Martins, A. B. D. S., Garcia, E. B., & Ferreira, L. M. (2022). Review of articulated elbow orthotics for joint stiffness rehabilitation. *Acta Ortopédica Brasileira*, 30(5), e254358.

[34] Deharde, M., & Patchel, K. (1997, August 19). Multi-functional dynamic splint.

[35] Johnson, G. R., Carus, D. A., Parrini, G., Marchese, S., & Valeggi, R. (2001). The design of a five-degree-of-freedom powered orthosis for the upper limb. *Proceedings of the Institution of Mechanical Engineers, Part H: Journal of Engineering in Medicine*, 215(3), 275-284.

[36] Bahadir, C., Akanirmak, Ü., Bahadir, E., Karacan, I., Şahin, Z., & Korkmaz, Ö. (2005). Hemiplejik hastalarda Bobath askısının fonksiyonel parametreler ve omuz subluksasyonu üzerine etkisi. *Haydarpaşa Numune Eğitim ve Araştırma Hastanesi Tıp Dergisi*, 45(2), 66- 70.

[37] Vanderniepen, I., Van Ham, R., Van Damme, M., & Lefeber, D. (2008, October). Design of a powered elbow orthosis for orthopaedic rehabilitation using compliant actuation. *In 2008 2nd IEEE RAS & EMBS International Conference on Biomedical Robotics and Biomechatronics* (pp. 801-806). IEEE.

[38] Schulz, S., Pylatiuk, C., Kargov, A., Gaiser, I., Schill, O., Reischl, M., ... & Rupp, R. (2009). Design of a hybrid powered upper limb orthosis. *In World Congress on Medical Physics and Biomedical Engineering, September 7-12, 2009, Munich, Germany: Vol. 25/9 Neuroengineering, Neural Systems, Rehabilitation and Prosthetics* (pp. 468-471). Springer Berlin Heidelberg.

[39] Kesmezacar, H., & Sarikaya, İ. A. (2010). Konservatif tedavi edilen basit dirsek çıkıklarının sonuçları. *Acta Orthop Traumatol Turc*, 44(3), 199a205.

[40] Pau, J. W., Xie, S. S., & Pullan, A. J. (2012). Neuromuscular interfacing: Establishing an EMG-driven model for the human elbow joint. *IEEE Transactions on biomedical engineering*, 59(9), 2586-2593.

[41] Bonutti, P. M., Bonutti, B. P., Ruholl, K. R., & Phillips, G. A. (2009, January 29). Orthosis apparatus and method of using an orthosis apparatus.

[42] Cempini, M., Giovacchini, F., Vitiello, N., Cortese, M., Moisé, M., Posteraro, F., & Carrozza, M. C. (2013, July). NEUROExos: A powered elbow orthosis for post-stroke early neurorehabilitation. *In 2013 35th Annual International Conference of the IEEE Engineering in Medicine and Biology Society (EMBC)* (pp. 342-345). IEEE.

[43] Ripel, T., Krejsa, J., Hrbacek, J., & Cizmar, I. (2014). Active elbow orthosis. *International Journal of Advanced Robotic Systems*, 11(9), 143.

[44] Vitiello, N., Cempini, M., Crea, S., Giovacchini, F., Cortese, M., Moise, M., ... & Carrozza, M. C. (2016). Functional design of a powered elbow orthosis toward its clinical employment. *IEEE/ASME Transactions on Mechatronics*, 21(4), 1880-1891.

[45] Herrnstadt, G., & Menon, C. (2016). Voluntary-driven elbow orthosis with speed-controlled tremor suppression. *Frontiers in bioengineering and biotechnology*, 4, 29.

[46] Ataoğlu, B., Ayanoğlu, T., Elshan, N., Özer, M., Çetinkaya, M., & Eyvazov, K. (2017). Basit Dirsek Çıkıklarında Kapalı Redüksiyon ve Erken Rehabilitasyon Sonuçlarımız. *Özgün Araştırmalar/Original Investigations*, 128.

[47] Cilaci, T., Gözaydinoğlu, Ş., & Uğurlu, Ü. (2018). Rijid Kontraktürleri Olan Lokalize Skleroderma Tanılı Bir Hastanın Rehabilitasyonu. *Bezmialem Science*, 6(4).

[48] Murugan, S. R., Raja, K. S., Prakash, K., & Naveenramkumarb, L. (2018). Rapid prototyping of elbow orthosis in biomedical application. *Int J Adv Res Eng Sci Technol*, 4, 275-280.

[49] Wee, J., Shank, T. M., Castro, M. N., Ryan, L. E., Costa, J., & Rahman, T. (2019, June). Elbow flexion assist orthosis for arthrogryposis. *In 2019 IEEE 16th International Conference on Rehabilitation Robotics (ICORR)* (pp. 494-498). IEEE.

[50] Bancud, K., Kutilek, P., & Krivanek, V. (2019, September). Design of powered wearable elbow brace for rehabilitation applications at clinic and home. *In 2019 European Conference on Mobile Robots (ECMR)* (pp. 1-6). IEEE.

[51] Minh, V. T., Tamre, M., Safonov, A., Kovalenko, P., & Monakhov, I. (2020). Design and implementation of a mechatronic elbow orthosis. *Mechatronic Systems and Control*, 48(4), 231-238.

[52] Dindorf, R., & Wos, P. (2020). Using the bioelectric signals to control of wearable orthosis of the elbow joint with bi-muscular pneumatic servo-drive. *Robotica*, 38(5), 804-818.

[53] Bonutti, P. M., Bonutti, B. P., Ruholl, K. R., & Phillips, G. A. (2019, March 5). Pronation/supination orthosis and method.

[54] Nikolaev, V. F., Golovin, M. A., Kornil'ev, N. S., & Lityakshev, N. A. (2020, January). Development of an elbow orthotic with elastic elements and distance adaptation control system. *In 2020 IEEE Conference of Russian Young Researchers in Electrical and Electronic Engineering (EIConRus)* (pp. 151-153). IEEE.

[55] Golovin, M. A., & Kornilev, N. S. (2021, May). Development Of An Elbow Orthotic With Elastic Elements. *In Assistive Technology* (Vol. 33, No. 3, pp. 158-159). 530 Walnut Street, STE 850, Philadelphia, PA 19106 USA: Taylor & Francis INC.

[56] Demirsoy, M. S., Kutlu, M. Ç., & Mansour, M. (2022). PID Kontrollü IoT Haberleşme İle Android Tabanlı Egsersiz Takibi. *Journal of Smart Systems Research*, 3(2), 70-80.

[57] Rodriguez, V., Sanchez, L., Palomares, R., & Cornejo, J. (2022, August). Ergonomic bio-design and motion simulation of a mechatronic orthosis system for elbow rehabilitation. *In 2022 IEEE XXIX International Conference on Electronics, Electrical Engineering and Computing (INTERCON)* (pp. 1-4). IEEE.

[58] Lavrenko, I., & Lebedynskyi, B. (2022). Determination of the stress-strain state of the structural elements of the elbow orthosis prototype. *International Science Journal of Engineering & Agriculture*, 1(3), 29-36.

[59] Arcos Rosero, J. D., Bolaños Rosero, D. C., Alape Realpe, L. F., Solis Pino, A. F., & Roldán González, E. (2022). Mechatronic Design of a Prototype Orthosis to Support Elbow Joint Rehabilitation. *Bioengineering*, 9(7), 287.

[60] Said, R. R., Yong, W. Q., Heyat, M. B. B., Ali, L., Qiang, S., Ali, A., ... & Wu, Z. (2022). Research Article Design of a Smart Elbow Brace as a Home-Based Rehabilitation Device.

[61] Petrov, E., Angelova, S., Raykov, P., & Paunski, Y. (2023). Autonomous Controller for an Active Elbow Orthosis. *In Proceedings of the International Scientific Conference "Robotics & Mechatronics 2023"* (pp. 1–4).